Bifurcation, Catastrophe, and Turbulence

E. C. Zeeman*

Introduction

Bifurcation occurs in a parametrised dynamical system when a change in a parameter causes an equilibrium to split into two. Catastrophe occurs when the stability of an equilibrium breaks down, causing the system to jump into another state. The elementary theory concerns dynamical systems with steady state equilibria (point attractors), and the non-elementary theory concerns systems with dynamic equilibria (periodic attractors and strange attractors). In the elementary case Thom [72] has used singularities to classify both bifurcation and catastrophe, and this has led to a great variety of applications [22]. We illustrate the contrasting styles of application in biology and physics by describing two recent examples. The first is a model by Seif [59] concerning hyperthyroidism, and the second is a model by Schaeffer [58] concerning Taylor cells in fluid flow.

In the non-elementary theory there is no classification yet, but Ruelle and Takens [51] have suggested using strange attractors to model the onset of turbulence. We describe some strange attractors and strange bifurcations, and discuss some of their properties that resemble turbulence, such as stability yet sensitive dependence on initial condition, and the broad band frequency spectra similar to those observed by Swinney and Gollub [67]. It is a pleasure to acknowledge my debt to David Rand for many discussions.

1. Elementary Examples

In this section we illustrate the difference between bifurcation and catastrophe by two simple examples and explain the relationship between them

* Department of Mathematics, University of Warwick, Coventry, England.

by a third example containing the first two. We draw attention to the important properties of stability, locality and symmetry. In the following two sections we shall give definitions, and explain how these simple examples typify the situation in higher dimensions.

1.1. The Pitchfork Bifurcation. This is the simplest example of a bifurcation, and has a canonical equation

$$\dot{x} = bx - x^3.$$

Here x is a real variable and b is a real parameter; $\dot{x}$ denotes dx/dt. The equilibrium set M is given by $bx - x^3 = 0$, and is shown in Figure 1. For

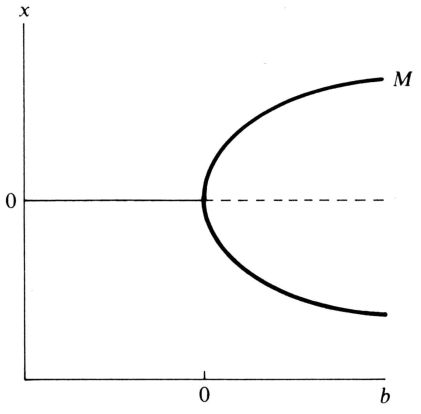

Figure 1

$b < 0$ there is a unique attractor (or stable equilibrium) at $x = 0$; for $b > 0$ there are two attractors at $x = \pm\sqrt{b}$, separated by a repellor (or unstable equilibrium) at $x = 0$. In Figure 1 the repellors are shown dotted. Therefore if the parameter is increased from negative to positive the attractor bifurcates at $b = 0$.

The pitchfork is unstable and local, as we shall now explain. It is *unstable* because there exist arbitrarily small perturbations with a topologically different equilibrium set (see Definition 2.2 below). For example the perturbation

$$\dot{x} = \varepsilon + bx - x^3, \qquad \varepsilon > 0,$$

breaks M into two components as shown in Figure 2. The component containing the unique attractors when $b < 0$ is called the *primary branch* because if b is increased from negative to positive the system will follow this branch. The attractors on the primary branch are called *primary modes*, and those on the other component are called *secondary modes*. The instability of the pitchfork can be analysed by unfolding it; here *unfolding* means adding

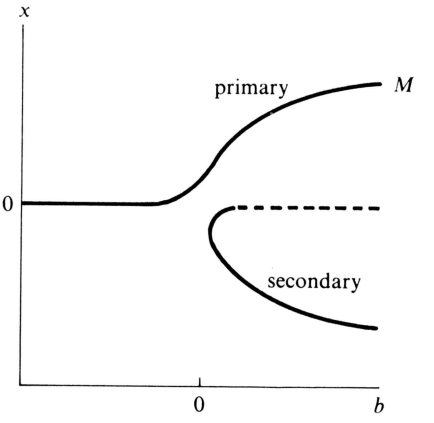

Figure 2

more parameters to make it stable. We shall see in 1.3 below that one more parameter is sufficient.

Meanwhile the pitchfork is *local* because it possesses an organising centre; here an *organising centre* means a point where the local dynamics is equivalent to the global dynamics of the whole system (see definition 2.3). The advantage is that the global dynamics can then be analysed locally at the organising centre. In the pitchfork the organising centre is the origin $x = b = 0$.

1.2. The Catastrophic Jump. The catastrophic jump PQ shown in Figure 3 has a beginning P and an end Q. The beginning P is a fold catastrophe, where an attractor and a repellor coalesce and disappear. The end Q is another attractor. The dynamical system illustrated in Figure 3 has the equation

$$\dot{x} = a + 3x - x^3,$$

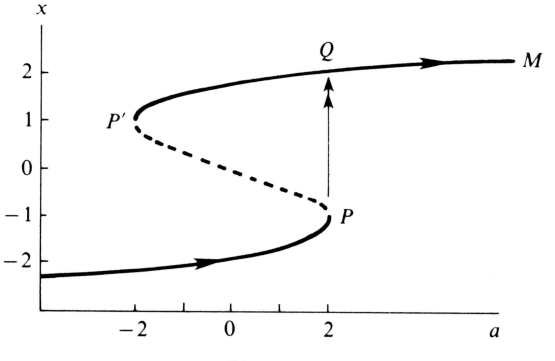

Figure 3

where the variable is x, and the parameter is a. For $|a| > 2$ there is a unique attractor, and for $|a| < 2$ there are two attractors separated by a repellor. The equilibrium set M is the curve given by $a + 3x - x^3 = 0$, and this has folds at $P = (2, -1)$ and $P' = (-2, 1)$. If the parameter is increased from negative to positive the system follows the lower attracting branch of M until it reaches $a = 2$ where it jumps from P to $Q = (2, 2)$, and it then follows the upper attracting branch. In this particular example there is hysteresis if the parameter is reduced again, because the return jump takes place at P', at a different parameter value $a = -2$. Not all jumps show hysteresis because there may not be a return jump; for instance, in Figure 2 a decrease in b causes a jump from the secondary to the primary mode, but there is no return jump if b is increased again.

In contrast to the pitchfork bifurcation the catastrophic jump is stable and non-local. *Stable* means that sufficiently small perturbations have equivalent M (see definition 2.2) and hence an equivalent jump. Meanwhile it is *non-local* because any analysis of the dynamics must involve both the taking-off point P and the landing point Q, and so there is no organising centre for the whole jump. It is true that the fold catastrophe by itself is local because it has an organising centre at P, but this would be an incomplete analysis of the global jump PQ.

Remark. The difference between local and global helps to explain why bifurcation theory is older than catastrophe theory. A local system can be linearised at the organising centre and treated as an eigenvalue problem; it can be analysed both quantitatively and qualitatively by examining the higher order terms of the Taylor expansion at the organising centre, using the methods of classical analysis. By contrast a non-local system may have to be tackled by methods of topology or modern global analysis, and may yield only qualitative rather than quantitative properties. Thus catastrophe theory had to wait for the development of twentieth-century topology, whereas bifurcation theory already had at its disposal nineteenth-century analysis.

On the other hand some non-local systems can be localised by identifying them with sections of a higher dimensional local system, with a hidden organising centre, as illustrated by the next example.

1.3. The Cusp Catastrophe. This is the next simplest elementary catastrophe after the fold, and has a canonical equation

$$\dot{x} = a + bx - x^3,$$

where x is the variable, and a, b are parameters. The equilibrium set is the surface M shown in Figure 4. The bifurcation set B is the image in the parameter space of the folds of M, and is the cusp $27a^2 = 4b^3$. For parameter points outside the cusp there is a unique attractor, and for parameter points inside the cusp there are two attractors separated by a repellor. In Figure 4

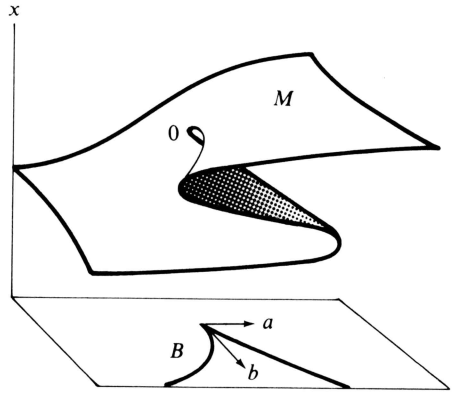

Figure 4

the shaded middle sheet repels, while the rest of M attracts. In applications a is sometimes called a *normal* factor, because it is correlated with x, and b is called a *splitting* factor, because it splits the attractor surface apart.

The cusp catastrophe is both stable and local, and contains both the previous examples as sections. The pitchfork in Figure 1 is the section $a = 0$, and hence the cusp catastrophe is its unique unfolding.* The perturbation in Figure 2 is the section $a = \varepsilon$. The jump in Figure 3 is the section $b = 3$. The origin 0 is the organising centre, and any section through 0 is unstable and local, like the pitchfork. Meanwhile, any section not through 0 that cuts the cusp transversally is stable and non-local because it contains a jump; we call 0 the *hidden* organising centre of these sections. Summarising: the local analysis of the cusp catastrophe at 0 elucidates the global dynamics of both pitchfork and jump, and reveals their interrelationship.

1.4. Symmetry. The pitchfork is symmetrical with respect to change of sign of x, but the cusp is not. We therefore call the b-parameter *symmetric* and the a-parameter *asymmetric*. Similarly any linear combination of a, b is asymmetric, and so the pitchfolk is the maximal symmetric section of the cusp.

In some problems the idealised model is symmetric, while the real model is represented by an asymmetric perturbation. For example the ideal elastic beam can be modelled by a pitchfork with b representing compression and x the resulting buckling [76]. The ideal beam is symmetric because it can buckle equally well up or down, but a real beam is liable to contain imperfections that make it behave like the asymmetric perturbation in Figure 2; hence it will always buckle the same way when compressed because it has to follow the primary branch. Summarising the procedure for such problems: represent the idealised problem by a symmetric bifurcation, unfold it, take

* An unfolding is unique up to equivalence [33, 72, 76]. Golubitsky and Schaeffer [16, 17] obtain a 1-dimensional higher unfolding because they retain b as a distinguished parameter.

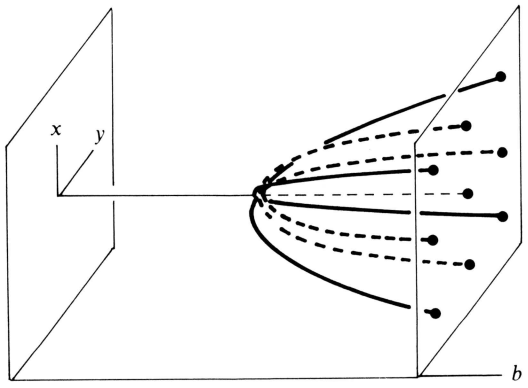

Figure 5

the maximal symmetric section, perturb it in an asymmetric direction, and then take the primary branch.

Of course, in the above special case the pitchfork turned out to be the same as the maximal symmetric section of its unfolding, but in the general case the latter may be larger. For example, consider the double-pitchfork shown in Figure 5 and given by the equations

$$\dot{y} = by - y^3$$
$$\dot{z} = bz - z^3$$

where y, z are variables and b is a parameter. Notice that b is a symmetric parameter with respect to changes of sign of both y and z. The double-pitchfork unfolds to the double-cusp with 8 parameters, of which 3 are symmetric and 5 asymmetric. One of the symmetric parameters is modal, and can be ignored for technical reasons [5, 10, 17, 27, 76]. Therefore the maximal symmetric section is given by adding the other symmetric parameter a, which has the effect of pulling the two pitchforks apart along the b-axis:

$$\dot{y} = (b + a)y - y^3$$
$$\dot{z} = (b - a)z - z^3.$$

Perturbing in the direction of an asymmetric parameter c and taking the primary branch will give a stable non-local equilibrium surface M over the (a, b)-plane, whose shape will depend on c. An example is shown in Figure 13 below.

2. Stability and Organising Centres

In this section we give the definitions of stability and organising centre for general flows, and in the next section we specialise to the elementary theory.

Let X be a manifold and ϕ a flow on X. Here a *flow* means a C^∞-map

$\phi\colon \mathbb{R} \times X \to X$, $\phi(t, x) = \phi^t x$, such that $\{\phi^t\}$ is a group action of $\mathbb{R}$ on X. The *ϕ-orbit* through x is $\phi(\mathbb{R} \times x)$. ϕ is the solution of a differential equation on X.

2.1. Definition of Nonwandering set. Call a point $x \in X$ *nonwandering* if, $\forall$ neighbourhood N of x, $\forall t \in \mathbb{R}$, $\exists s > t$, such that $\phi^s N$ meets N. The set of all such is called the *nonwandering set* Ω. Let M denote the *fixed point set* (or equilibrium set) of ϕ. In the elementary case $\Omega = M$, but in the general case $\Omega \supset M$ because Ω will also contain periodic orbits, strange attractors, etc. (See Sections 6 and 7 for examples.) Since all orbits flow to Ω the asymptotic behaviour of ϕ is determined by Ω.

Parameters. Let C be a parameter manifold. Let ϕ be a flow on X parametrised by C; here ϕ is a C^∞-map $\phi\colon C \times \mathbb{R} \times X \to X$, $\phi(c, t, x) = \phi_c(t, x)$, and ϕ_c is a flow on X, $\forall c \in C$. Define the parametrised nonwandering set

$$\Omega = \bigcup (c \times \Omega_c) \subset C \times X,$$

where Ω_c is the nonwandering set of ϕ_c, $\forall c \in C$. Let $\chi\colon \Omega \to C$ be induced by the projection $\pi\colon C \times X \to C$. For example, in the cusp catastrophe (1.3 above) $\Omega = M$, the parametrised fixed point set, and χ is the projection onto $\mathbb{R}^2$ shown in Figure 4.

2.2. Definition of Stability. Given flows ϕ, ϕ' on X, X' parametrised by C, C' with nonwandering sets Ω, Ω' define them to be *equivalent*, written $\phi \sim \phi'$, if $\exists$ a homeomorphism α throwing orbits to orbits, and a diffeomorphism γ, such that the following diagram commutes:

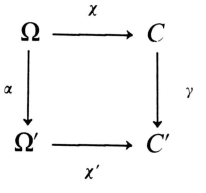

Define ϕ to be *stable* if perturbations are equivalent. Here a *perturbation* of ϕ means the solution of a differential equation sufficiently close to that for ϕ.

Remark. The above definition is usually called Ω-stability to distinguish it from structural stability, in which the homeomorphism α and the commutativity extend to the whole of $C \times X$. Structural stability was first introduced by Andronov and Pontryagin [3], and the weaker definition of Ω-stability was later introduced by Smale [64] to embrace a larger class of flows. Neither definition is generic, because Ω-stable flows are not dense [2]. It was originally hoped to find a generic definition, but hopes dwindled as more examples were discovered. Meanwhile the importance of structural stability and Ω-stability was emphasised by theorems characterising them [39, 44, 48, 49, 65]. For simplicity of exposition we have chosen Ω-stability in this paper.

In elementary theory the situation is much tidier because the definition is generic, and for low dimensions of C one can sharpen α to be a diffeomorphism, as we explain in the next section. For more detailed discussions of stability see [1, 30, 64, 72, 73].

2.3. Definition of Organising Centre. Given a flow ϕ on X parametrised by C we call $P \in \Omega$ an *organising centre* for ϕ if $\exists$ arbitrarily small neighbourhoods Ω', C' of P, χP in Ω, C, a homeomorphism α throwing orbits to orbits, and a diffeomorphism γ, such that the following diagram commutes:

$$\begin{array}{ccc} \Omega', P & \xrightarrow{\chi|\Omega'} & C' \\ \downarrow{\scriptstyle \alpha} & & \downarrow{\scriptstyle \gamma} \\ \Omega, P & \xrightarrow[\chi]{} & C \end{array}$$

Call ϕ *local* if it has an organising centre.

2.4. Lemma. *The cusp catastrophe is stable and local.*

PROOF. For the stability see [76]; we verify here that it is local. The cusp is defined in 1.3 above and has $X = \mathbb{R}$, $C = \mathbb{R}^2$, and $\Omega = M \subset C \times X$ given by $a + bx - x^3 = 0$. Given $\varepsilon > 0$, let C' be the open disk $a^2 + b^2 < \varepsilon$, and let $M' = \chi^{-1}C'$. Define $\alpha\colon M' \to M$, $\gamma\colon C' \to C$ by

$$\alpha(a, b, x) = (s^3a, s^2b, sx)$$
$$\gamma(a, b) = (s^3a, s^2b), \qquad s = \sec \frac{\pi}{2\varepsilon}(a^2 + b^2).$$

This satisfies commutativity, and hence the origin is an organising centre. Notice that since this example is elementary α is not only a homeomorphism but also a diffeomorphism, and it extends to the ambient space.

2.5. Definition of Bifurcation Set and Catastrophe Set. Given a flow ϕ on X parametrised by C, let Ω_* denote the map $c \to \Omega_c$ from C to the space of closed sets of X, with the Hausdorff topology. Call a parameter point c *regular* if Ω_* is constant in a neighbourhood of c, up to equivalence. Define the *bifurcation set* B to be the set of non-regular points. Define the *catastrophe set* K to be the closure of the set where Ω_* is discontinuous. Therefore we have closed subsets

$$K \subset B \subset C.$$

A point in K is called a *catastrophe point* and a point in $B - K$ is called a

bifurcation point. Thus Ω_* is continuous in the neighbourhood of a bifurcation point, but discontinuous in the neighbourhood of a catastrophe point.

For example, the pitchfork Ω_* is continuous, so $K = \varnothing$ and the organising centre is a bifurcation point; that is why it is called the pitchfork bifurcation. By contrast, in the cusp catastrophe Ω_* is continuous at the organising centre but discontinuous elsewhere on the cusp, so $K = B$ and the organising centre is a catastrophe point; that is why it is called the cusp catastrophe rather than the cusp bifurcation. For a philosophical discussion see Thom [72].

3. Elementary Theory

In this section we explain Thom's density and classification theorem for elementary catastrophes.

3.1. Definition of Elementary. Given a flow ϕ on X, call ϕ *elementary* if there exists a Lyapunov function. Here a *Lyapunov function* means a C^∞-function $f\colon X \to \mathbb{R}$ that decreases strictly along orbits of ϕ. If ϕ is elementary the nonwandering set of ϕ is the critical set of f, given by $df = 0$, and the attractors of ϕ are the minima of f.

We now introduce parameters. Given a flow ϕ on X parametrised by C, call ϕ elementary if there exists a parametrised Lyapunov function f. Here f is a C^∞-function $f\colon C \times X \to \mathbb{R}$, $f(c, x) = f_c x$, such that f_c is a Lyapunov function for ϕ_c, $\forall c \in C$. Therefore

$$\Omega = M = \text{critical set of } f, \quad \text{given by } d_X f = 0.$$

Examples. Gradient flows are elementary; here a *gradient flow* means the solution of a gradient differential equation $\dot{x} = -\nabla f$, and this is elementary because f is a Lyapunov function. For instance, the cusp catastrophe is elementary because it is gradient:

$$\dot{x} = -\nabla_X f = -\frac{\partial f}{\partial x}, \quad \text{where } f = \tfrac{1}{4}x^4 - \tfrac{1}{2}bx^2 - ax.$$

Therefore $\Omega = M$ is given by

$$d_X f = \frac{\partial f}{\partial x} = x^3 - bx - a = 0.$$

Gradient-like flows are also elementary [64]. On the other hand, the examples in Sections 6 and 7 below are non-elementary because they contain periodic orbits.

Remark. The restriction to elementary theory is a severe restriction, but nevertheless there are many phenomena in which steady-state equilibria are predominant, and so the elementary theory does have wide application [15, 21, 22, 43, 72, 76]. In the elementary theory the asymptotic behaviour of the flow ϕ is determined by the critical set M of its Lyapunov function f, and so the mathematical trick is to switch attention from ϕ to f. This trick does have some limitations [19] but is adequate for most applications. The mathematical advantage of switching to functions is that we can sharpen the definition of stability and use results from singularity theory, as follows.

3.2. Definition of Stability of Functions. Given functions f, f' on X, X' parametrised by C, C' define them to be *equivalent*, written $f \sim f'$, if $\exists$ diffeomorphisms α, β, γ such that the diagram commutes:

$$\begin{array}{ccccc} C \times X & \xrightarrow{\pi \times f} & C \times \mathbb{R} & \xrightarrow{\pi} & C \\ \downarrow{\scriptstyle \alpha} & & \downarrow{\scriptstyle \beta} & & \downarrow{\scriptstyle \gamma} \\ C' \times X' & \xrightarrow{\pi \times f'} & C' \times \mathbb{R} & \xrightarrow{\pi} & C' \end{array}$$

This induces an equivalence of critical sets:

$$\begin{array}{ccc} M & \xrightarrow{\chi} & C \\ {\scriptstyle \alpha|M}\downarrow & & \downarrow{\scriptstyle \gamma} \\ M' & \xrightarrow{\chi'} & C' \end{array}$$

Therefore if f, f' are Lyapunov functions for the flows ϕ, ϕ' then

$$f \sim f' \Rightarrow \phi \sim \phi'.$$

Let $F = C^\infty(C \times X)$, the space of all C^∞-functions on X parametrised by C, with the Whitney C^∞-topology [76]. Given $f \in F$ call f *stable* if it has a neighbourhood of equivalents. If f is stable then its critical set M is a manifold the same dimension as C, and $\alpha \mid M$ above is a diffeomorphism.

Example. Morse functions are stable; here a *Morse function* means a function on $\mathbb{R}^n$ that is quadratic of rank n, and independent of the parameter C.

The cusp catastrophe has a stable Lyapunov function, $f = x^4 - 2bx^2 - 4ax$ (multiplying by 4 to get rid of fractions). The germ of f at the organising centre is x^4, and, conversely, f is the unique unfolding of its germ, up to equivalence. Here *unfolding* means stabilising by adding the minimum number of parameters. In this sense the cusp is uniquely determined by its germ. (For proofs see, for example, [76, Chapter 18].)

Analogous to the cusp there are 11 elementary catastrophes* for dim $C \leq 5$, determined by the germs x^3, x^4, x^5, x^6, x^7, $x^2y \pm y^3$, $x^2y + y^4$, $x^2y \pm y^5$, $x^3 + y^4$, and each one is stable and local. Moreover, this is a complete classification in the sense of Theorem 3.4 below. In order to state the classification theorem globally it is necessary to localise the definitions of equivalence and stability, as follows.

3.3. Definition of Local Stability. Given functions f, f' on X, X' parametrised by C, C', and points y, y' in $C \times X$, $C' \times X'$, define them to be *locally-equivalent*, written $(f, y) \sim (f', y')$, if $\exists$ neighbourhoods N, N' of y, y' such that $f|N \sim f|N'$. Given $f \in F$, where $F = C^\infty(C \times X)$, call f *locally-stable* if, $\forall y \in C \times X$, $\forall$ neighbourhood N of y, $\exists$ a neighbourhood V of f, $\forall f' \in V$, $\exists y' \in N$, such that $(f, y) \sim (f', y')$. Notice that stable implies locally-stable, but not conversely. Local-stability implies that the critical set M is a manifold, of the same dimension at C.

3.4. Theorem (Thom [72] and Mather [33]). *If* dim $C \leq 5$ *then locally-stable functions are dense in F. If f is locally-stable then at each point it is locally-equivalent to either a linear function, or a Morse function, or the product of an elementary catastrophe with a Morse function.*

For a proof see, for example, [31, 76 Chapter 18].

This theorem explains why the elementary catastrophes and their sections are so universal. As in 1.3, each elementary catastrophe has two types of section, depending upon whether or not the section goes through the organising centre. If it does then the section gives an unstable local bifurcation like the pitchfork. If it does not then the section will generically give a stable non-local system like the jump, consisting of a configuration of lower dimensional catastrophes. This configuration is determined by the hidden organising centre, hidden because it lies off the section. When such a configuration is observed it may be useful to look for a hidden organising centre, because the latter may provide an analysis of the dynamics, as illustrated in 5.4 below. Summarising: the identification of pitchfork and jump as sections of the cusp typifies the relationship between bifurcation and catastrophe in higher dimensions.

In the next two sections we illustrate the use of elementary catastrophe theory by describing two recent applications. The first is in medicine, and typifies applications in the biological or social sciences where the catastrophe is taken as a hypothesis. The second is in fluid mechanics, and typifies applications in the physical sciences where the singularity is derived from basic underlying assumptions, such as conservation laws or variational principles, etc.

* Thom's list of elementary catastrophes [72, 76] has been considerably extended to higher dimensions by Arnold [5], but the definitions have to be modified to allow for the appearance of modal parameters.

4. Hyperthyroidism

This is a model by Seif [59]. In normal individuals there is a hormone* chain:

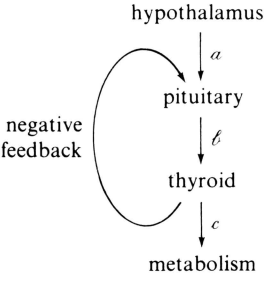

For instance, a sensation of cold would be registered in the brain by activity of the hypothalamus, causing a release of hormone a into the blood stream, which triggers the pituitary gland to release hormone b, which triggers the thyroid gland to release hormone c, which stimulates the metabolism throughout the body, changing chemical energy into heat. The negative feedback means that large c (in other words, a high concentration of c in the blood) causes the pituitary to stop releasing b. There are two ways this chain can go wrong, hypo and hyper, as follows.

4.1. Hypothyroidism. Hypothyroidism means too little c. This in turn causes large b due to lack of negative feedback. Also, every time the hypothalamus receives a stimulus and releases a in an attempt to get the metabolism going nothing happens, and so it continues to release a, reinforcing the large b. The typical cause of too little c is a lack of iodine, without which the thyroid cannot manufacture c. Typical symptoms of hypothyroidism are feelings of cold and sluggishness, and a tendency for the individual to grow fat. A cure is to inject c.

4.2. Hyperthyroidism. Hyperthyroidism means too much c. This in turn causes small b, due to the feedback. The typical cause is the presence of some immunoglobulin b^* in the blood that accidentally resembles b, and which the thyroid mistakes for b. Since b^* is always present in the blood the thyroid is permanently turned on to the production and release of c. The original appearance of b^* may have been triggered by some quite independent immunological response, but once triggered it is always present, thus inducing a permanent state of hyperthyroidism. Typical symptoms of hyperthyroidism are that the individual feels hot and irritable, becomes overactive and thin, develops bulbous eyeballs and a bulge in the neck called a goitre

* a = TRH(thyrotropic releasing hormone) = protirelin.
b = TSH(thyroid stimulating hormone) = thyrotropin.
c = index measuring thyroxine (T_4) and triiodothyronine (T_3).

due to the enlarged overactive thyroid. A temporary treatment is to inject drugs that interfere with the metabolism, thus counteracting the effect of large c. The permanent treatment is to remove or destroy some of the thyroid gland until what is left produces the desired amount of c.

Seif applied this standard treatment to 78 hyperthyroid patients, but found that although the treatment produced normal levels of b and c, and indeed cured two-thirds of his patients, the other third were apparently not properly cured because they began to display some of the opposite symptoms of hypothyroidism, such as the inability to react to cold.

4.3. Pituitary Failure. What had happened was that the pituitary was no longer responding to the a-hormone; evidently during the long period of high negative feedback, in a desperate attempt to stem the flood of c, the pituitary had given up releasing b, and consequently lost its response-ability. Seif measured this response-ability by injecting a standard dose of a and observing the resulting change in the level of b. Let $x = b_1/b_0$, where b_0 is the initial level, and b_1 the level twenty minutes after injection, which is the normal time for maximal response. He found that for normal individuals and for the successfully cured two-thirds x had mean 7, but for hyperthyroid patients and for the abnormal third of treated patients $x = 1$. For convenience we shall refer to the abnormal third by the single word *treated*. Figure 6 sketches the four types on the (b, c)-plane, and Figure 7 sketches their response to the injection of a.

Seif had collected 422 measurements during the diagnosis and treatment of 314 patients, but at this point he was stuck for a conceptually simple way to present, or think about, his data. That is until he happened to hear a lecture mentioning the cusp catastrophe, which he immediately recognised as relevant, because x was bimodal for some points in the (b, c)-plane but unimodal for others. The resulting model is shown in Figure 8.

4.4. Cure. The diagram immediately suggested the possibility of catastrophic jumps α and β. The jump α represents the onset of hyperthyroidism, and the jump β represents a possible cure for the treated patients. Their treatment so far is represented by the path HK in the parameter space, which

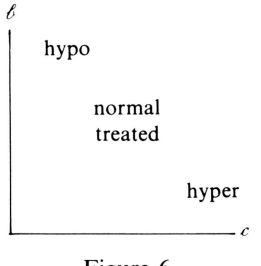

Figure 6

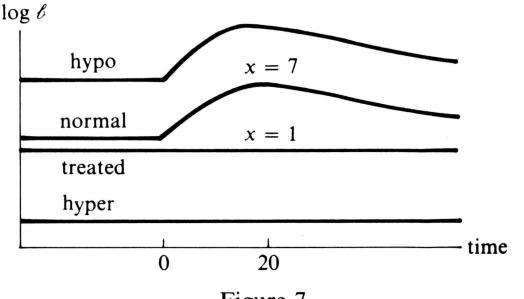

Figure 7

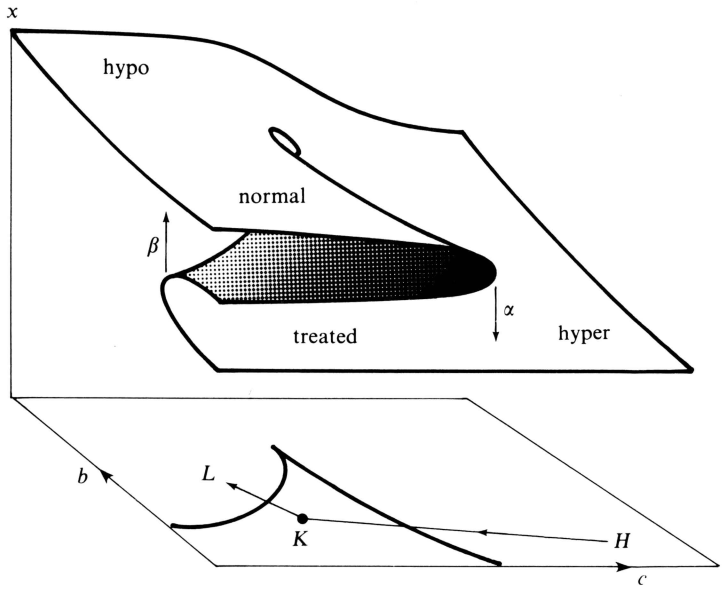

Figure 8

takes about 6 weeks, and is the slow change in the average levels of b, c resulting from the removal of some of the thyroid gland. The additional treatment would be to steer the patient along the path KL, until the left side of the cusp is crossed, where the patient will jump back to normal. This guiding of the patient through hypothyroidism takes about another 3 weeks and is achieved by drugs that stimulate the production of a by reducing the metabolism, and suppress the negative feedback by interfering with the production of c, thus inducing the pituitary to very gradually raise the average level of b. To Seif's delight this new additional treatment successfully cured the remaining third of his patients. Evidently the other two-thirds had cured themselves either by already crossing the left side of the cusp or by going round the top.

It could be argued that, having identified the pituitary as the culprit, the guiding of the patient through hypothyroidism would have been a logical way to try and cure the patient anyway, without reference to Figure 8. However without Figure 8 one would not have predicted the suddenness of the jump β, nor the stability of the patient's normality immediately after the jump. Therefore Figure 8 makes the monitoring of the additional treatment conceptually very easy, because all the doctor has to do is to make regular injection tests until he observes a jump in x, and he can then send the patient home cured. Going back to our original discussion at the beginning of the paper, of the relationship between the pitchfork and the jump, what was first observed in this application was the bifurcation, and what was successfully predicted as a result was the jump.

4.5. Data Fitting. The next step was to fit a cusp to the data. Theoretically (Theorem 3.4) the cusp surface is only differentially equivalent (Definition 3.2) to the standard surface (Example 1.3), but near the cusp point a linear fit is a good approximation. Therefore Seif assumed that, up to additive and multiplicative constants, the variable was log x, the normal factor was c, and the splitting factor $-b$; he calculated the constants by a least squares fit on x using an iterative computer programme. The resulting cusp lines are shown in Figure 9; the curvature of the right side is reversed due to the log-scale. Notice that, as anticipated from Figure 8, normal individuals are bounded on the right by the right side of the cusp, and the treated patients are bounded on the left by the left side of the cusp.

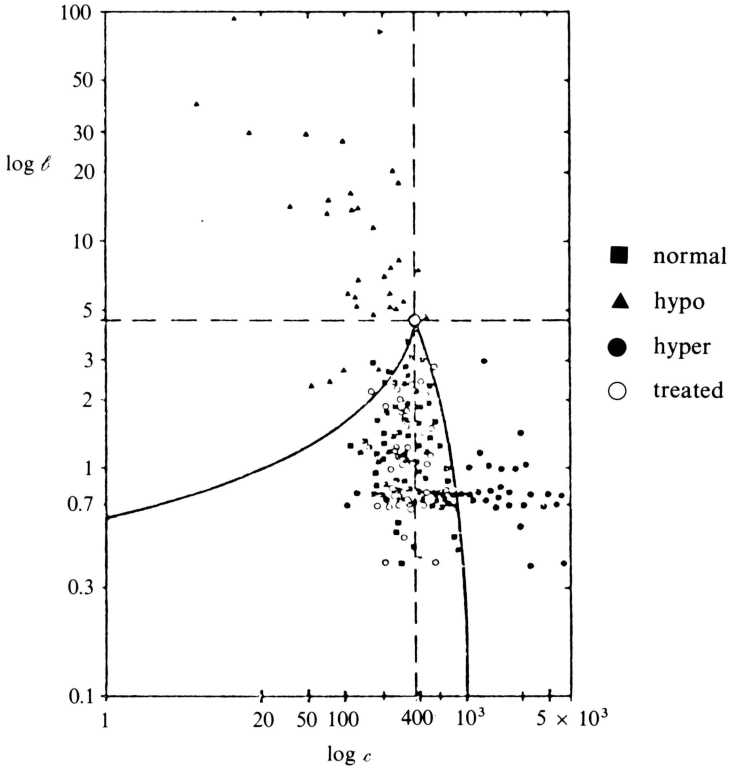

Figure 9 (Seif [59]).

4.6. Micro-Model. The next task was to explain the cusp, because a good model should not only provide a structural description at the phenomenological level, but also admit a reductionist explanation at the micro-level. Therefore Seif constructed a stochastic microscopic model of granule formation, stimulus-secretion, and diffusion, of the b-hormone in individual pituitary cells. He then showed that the resulting macroscopic behaviour of the

pituitary gland would have an equilibrium surface with the same formula that he had used for the data fitting. Therefore Figure 8 represents not only a distribution of patients, but also the behaviour of the pituitary gland.

4.7. Summarising. Seif's model is useful in five ways. Firstly, it provided a simple conceptual grasp of the problem. Secondly, it suggested a successful cure. Thirdly, it enabled the data to be fitted. Fourthly, it stimulated the construction of a micro-model, and provided an objective for the latter to explain. Fifthly, it provides a theoretical framework for ongoing research into the molecular substructure.

5. Taylor Cells

This is a model by Schaeffer [58] to explain the experimental results of Benjamin [6] in the classical Couette [11]–Taylor [71] problem in fluid mechanics (see Figure 10).

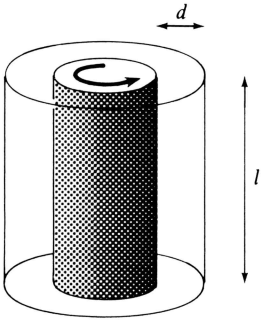

Figure 10

Water is placed between two vertical concentric cylinders, and the inner cylinder is rotated causing the fluid to rotate. We take as a parameter the Reynolds number R, which is proportional to the speed of the inner cylinder. For small R the fluid velocity field ξ is azimuthal, in other words all the streamlines are horizontal circles concentric with the cylinders. If the end effects are ignored (or equivalently if the cylinders are infinitely long) it is easy to calculate ξ from the Navier–Stokes equations [26]; ξ depends on the cylinder speed but turns out to be independent of viscosity, and is called Couette flow [11].

If R is increased then Couette flow becomes unstable; cells appear, called Taylor cells, and the fluid settles down into a new type of steady flow called Taylor flow [71]. Each cell is a horizontal solid torus of approximately square cross-section. Inside each cell the flow is spiral; there is one horizontal circular streamline in the interior of the cell and all the other streamlines

spiral round it. Alternate cells spiral clockwise and anticlockwise, as shown in Figure 11. The boundaries between the adjacent cells are horizontal, and alternate boundaries spiral inwards and outwards. Intuitively it is the outward spiralling boundaries that are being driven by centrifugal force, and they in turn drive the cells.

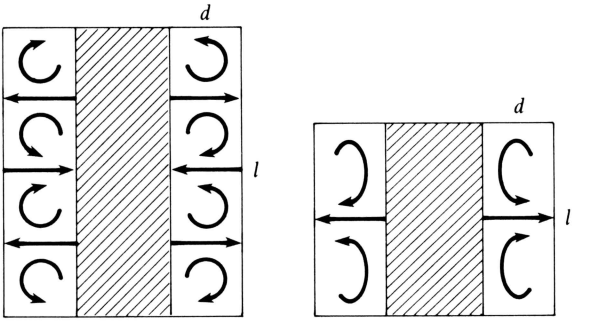

Figure 11

We now want to take the end effects into account. Define the *aspect ratio* to be $\rho = l/d$, where l is the length of the cylinders and d the clearance between them. Since the cells are approximately square in cross-section, the number of cells is approximately equal to ρ. At the ends of the cylinders the velocity is zero due to friction, and so in the boundary layers at the ends the velocity is small; therefore the centrifugal force is small, and this biases the end layers to spiral inwards. This bias normally causes an even number of cells to form, as in Figure 11. If, however, we make $\rho = 3$, then the poor fluid does not know whether to form 2 cells or 4 cells, and this is the phenomenon we want to discuss.

5.1. Experimental Data. Benjamin [6] performed the experiment, taking as parameters the Reynolds number R and the aspect ratio ρ. He found that if ρ is fixed and R varied then at certain critical values of R the fluid jumps from 2 cells to 4 cells or vice versa. By "jump" we mean that on one side of the critical value both configurations of cells are stable, but if R is moved across the critical value then one of the configurations loses its stability, and the fluid will settle down into the other; the time it takes to jump will depend upon the viscosity. Let C denote the region of the parameter plane in which the experiment is valid. Benjamin plotted the observed jump points in C and obtained the cusp-shaped bifurcation curve in Figure 12.

Theoretically, if we choose a suitable variable v and plot v over C then we should obtain the cusp catastrophe surface M shown in Figure 13. For example, let v be the inward radial component of the velocity at a point halfway up the cylinders midway between them. This is a suitable variable because $v < 0$ in the 2-cell flow, $v = 0$ in the Couette flow, and $v > 0$ in the

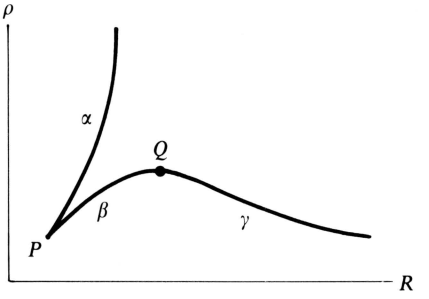

Figure 12

4-cell flow, as can be seen from Figure 11. Therefore for large R the lower sheet of M in Figure 13 represents the 2-cell mode and the upper sheet the 4-cell mode.

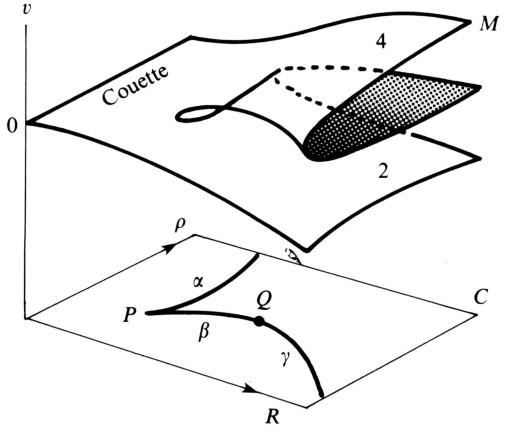

Figure 13

5.2. Digression on the Meaning of "Suitable." Let X be the ∞-dimensional space of all possible fluid velocity fields in the apparatus. The Navier–Stokes equations determine an evolution equation E on X, parametrised by C. The equilibrium set of E is a cusp catastrophe surface $M \subset C \times X$. Let $v\colon X \to \mathbb{R}$ be a function, for example some measurement of the velocity field. We call v a *suitable* variable if the composition

$$M \xrightarrow{\subset} C \times X \xrightarrow{1 \times v} C \times \mathbb{R}$$

is an embedding. Notice that $1 \times v$ crushes the ∞-dimensional space $C \times X$ down onto the 3-dimensional space $C \times \mathbb{R}$, but does not crush M. Notice also that the dynamic E sits up in $C \times X$, and that there is no dynamic in $C \times \mathbb{R}$, only the equilibrium set M and the catastrophic jumps, as follows.

5.3. Qualitative Description. The two important points of the bifurcation set are the cusp point P, and the point Q where the tangent is parallel to the R-axis. These points divide the bifurcation set into three arcs α, β, γ as shown in Figure 12. The reason why these points are important is that in each experiment ρ is fixed and so the variation of R is represented by a section $\rho =$ constant; all such sections are stable except those through P and Q, where the equivalence class of section changes, as shown in Figure 14. If

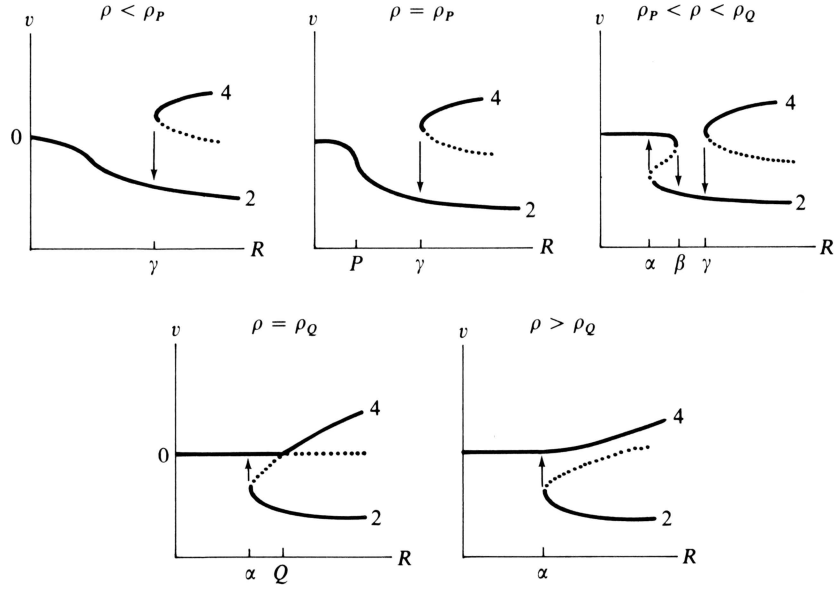

Figure 14

$\rho < \rho_P$ then the 2-cell mode is primary and the 4-cell mode secondary; if $\rho > \rho_Q$ the situation is reversed. Unstable modes are shown dotted. If $\rho_P < \rho < \rho_Q$ there is a hysteresis on the primary branch between an incipient 4-cell mode and the 2-cell mode, while the 4-cell mode is secondary. If the system is in the 2-cell mode and R is decreased across the arc α then it will jump into the 4-cell mode. The reverse jump occurs if R is increased across β or decreased across γ. A similar phenomenon happens in embryology [76].

5.4. Mathematical Analysis. Benjamin was unable to solve the Navier–Stokes equations because of the difficulties presented by the boundary conditions at the ends of the cylinders. Taylor's original solution [76] had avoided this difficulty by assuming infinitely long cylinders and proceeding as follows. For small R the Couette flow ξ is the unique attractor of the evolution equation E on X, and so he used (R, ξ) as an organising centre; by linearising E at the organising centre he was able to calculate the critical Reynolds number R_c where ξ becomes unstable, and express the Taylor flow

as a perturbation of ξ. The reason that Benjamin was unable to follow the same procedure was that Figure 13 is non-local since there are two qualitatively significant points P and Q.

Schaeffer [58] realised this and had the brilliant idea of seeking a *hidden* organising centre. We sketch his procedure briefly, as follows. His first trick was to introduce a hidden parameter τ to represent the friction at the ends of the cylinders. Then $\tau > 0$ in the experiment, but $\tau = 0$ at the organising centre, and so Figure 13 will turn out to be a section of a higher dimensional catastrophe not through the organising centre. This explains why it is stable and non-local (see 3.4). When $\tau > 0$ the fluid velocity at the ends of the cylinder has to vanish due to friction, but when $\tau = 0$ it need not vanish. This has the great advantage of allowing Couette flow ξ to become a valid solution of the equations, and so Schaeffer was then able to follow Taylor's trick of making it the organising centre.

Let R_2 be the critical value of R at which ξ becomes unstable with respect to the Taylor 2-cell flow. Taylor [71] showed that the 2-cell flow is represented by a perturbation $\xi + \eta y$, where η is a velocity field orthogonal to ξ, and y is a real variable obeying a pitchfork bifurcation with organising centre $(R_2, 0)$, as shown in Figure 15. If $R < R_2$ then ξ is an attractor, given

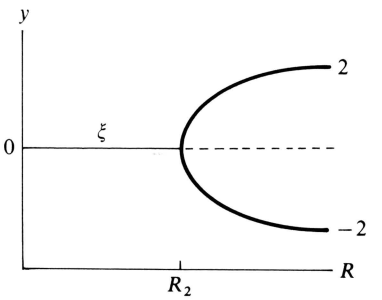

Figure 15

by $y = 0$. If $R > R_2$ then the upper branch in Figure 15 is an attractor, representing the 2-cell flow shown in Figure 11, and the lower branch is another attractor representing the similar flow spiralling in the opposite direction, with both ends spiralling inwards rather than outwards (which is equally valid when $\tau = 0$ due to the absence of any frictional bias). Similarly, let R_4 be the critical value at which ξ becomes unstable with respect to the 4-cell flow, and let $\xi + \zeta z$ be the corresponding perturbation of ξ, where ζ is a velocity field orthogonal to ξ, and z a real variable obeying another pitchfork with organising centre $(R_4, 0)$.

Now consider the double perturbation $\xi + \eta y + \zeta z$. If $R_2 \neq R_4$ the two pitchforks have different organising centres, and so the next trick is to make $R_2 = R_4$, so as to bring them together into a double-pitchfork (see Figure 5). This trick is possible because R_2 and R_4 are functions of the aspect ratio ρ,

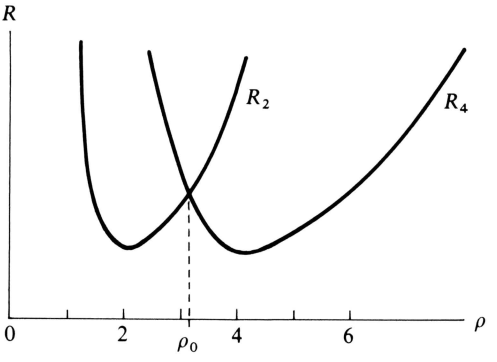

Figure 16

as shown in Figure 16. R_2 has a minimum near 2, R_4 has a minimum near 4, and their graphs cut at ρ_0, say, near 3. Putting $\rho = \rho_0$ makes $R_2 = R_4$.

In the classical language this makes the problem into a double eigenvalue problem. In the language of singularity theory: unfold the double-pitchfork into the double-cusp catastrophe, restrict to the maximal symmetric section, perturb in the direction of the asymmetric parameter τ, and take the primary branch M (see 1.4). Now ρ is the other symmetric parameter besides R, and so M will be a connected surface in the 4-dimensional (R, ρ, y, z)-space. Finally, let $v = z - y$. Then v is a suitable variable (in the sense of 5.2) and so the map $(y, z) \mapsto v$ induces an embedding of M in the 3-dimensional (R, ρ, v)-space, recovering Figure 13. Of course, v is not the same variable as we had before, but the surface is equivalent.

The reason for restricting to the maximal symmetric section is that, when $\tau = 0$, if $\xi + \eta y + \zeta z$ is an attractor, then $\xi \pm y\eta \pm \zeta z$ will also be attractors; therefore the equilibrium set is symmetric with respect to change of sign of y and z. We need to explain, however, why we have ignored the 3-cell modes, which are equally valid when $\tau = 0$, and which bifurcate off ξ at a lower Reynolds number than $R_2 = R_4$ when $\rho = \rho_0$. They can be ignored because, when $\tau > 0$, the frictional bias towards inwards spiralling at both ends has the effect of disconnecting both 3-cell modes from the primary branch M, so that they become secondary modes that will not be observed without special initial conditions. Similarly the lower branches of both the 2-cell and 4-cell pitchforks are disconnected from M, leaving in M only the two modes y, $z > 0$ illustrated in Figure 11.

5.5. Summary. Schaeffer found a hidden organising centre at which the Navier–Stokes equations could be analysed to provide a theoretical explanation for Benjamin's experimental data. It would be even more interesting if his techniques could be extended to non-elementary theory to embrace the periodic, quasi-periodic, and turbulent motion at higher Reynolds numbers [12, 13, 67]. This is the theme of the rest of the paper.

6. Non-elementary Examples

In this section we illustrate the difference between bifurcation and catastrophe in non-elementary theory by describing some examples analogous to those in Section 1. The main difference is that here the flows contain periodic attractors, or limit cycles. We define the Bowen–Ruelle measure [9] on an attractor and show that it can vary continuously even when there is a catastrophic Ω-explosion. For more examples of bifurcation see [1, 32, 36, 68, 69].

6.1. The Hopf Bifurcation [25]. This has canonical equations

$$\dot{\theta} = 1$$

$$\dot{r} = br - r^3$$

where (r, θ) are polar coordinates for the space $\mathbb{R}^2$, and b is a parameter. When $b \leq 0$ the origin O is an attractor; when $b > 0$ it becomes a repellor, and a new periodic orbit α appears at $r = \sqrt{b}$ (see Figure 17). Therefore the nonwandering set is

$$\Omega_b = \begin{cases} O, & b \leq 0 \\ O \cup \alpha, & b > 0. \end{cases}$$

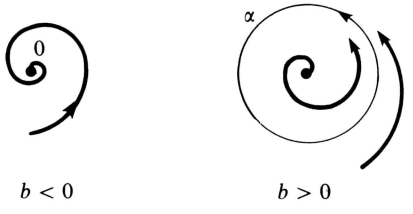

Figure 17

By Hopf's theorem [25, 32] this example is stable and local, with organising centre at the origin, $r = b = 0$. Since Ω_b depends continuously on b, the point $b = 0$ is a bifurcation point.

6.2. An Ω-Explosion. Let the state-space be the unit circle α, with coordinate θ, $0 \leq \theta < 2\pi$, and let a be a parameter. Consider the equation

$$\dot{\theta} = a - \cos\theta.$$

When $-1 < a < 1$ there is a repellor S at $\theta = \cos^{-1} a$, and an attractor A at $\theta = -\cos^{-1} a$. When $a = 1$ these two fixed points coalesce into a single fixed point N at $\theta = 0$, and when $a > 1$ they disappear (see Figure 18). Therefore the nonwandering set is

$$\Omega_a = \begin{cases} A \cup S, & -1 < a < 1 \\ N, & a = 1 \\ \alpha, & a > 1. \end{cases}$$

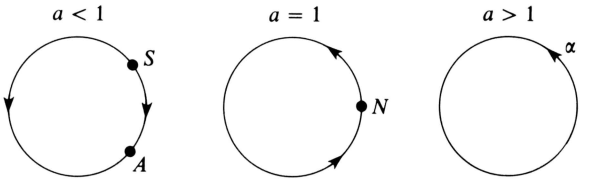

Figure 18

Although locally there is a fold catastrophe at N, globally there is a Ω-explosion from the point N to the whole circle α. Since Ω_a is discontinuous at $a = 1$ the latter is a catastrophe point. Therefore qualitatively we may call this example a catastrophe, but quantitatively there are measure-theoretic arguments for calling it a bifurcation, as we shall see in 6.6 below.

Since there is no organising centre, this example is stable and non-local. However, we can find a hidden organising centre, as follows. First embed the unit circle in $\mathbb{R}^2$ and extend the equation to:

$$\dot{\theta} = a - r\cos\theta$$

$$\dot{r} = r - r^3.$$

This preserves the attractor A, converts the previous repellor S into a saddle, and introduces a repellor R at the orign. When $a = 1$ the attractor coalesces with the saddle at the saddlenode N, and when $a > 1$ they disappear leaving only the attractor α and repellor R (see Figure 19). The extended system is

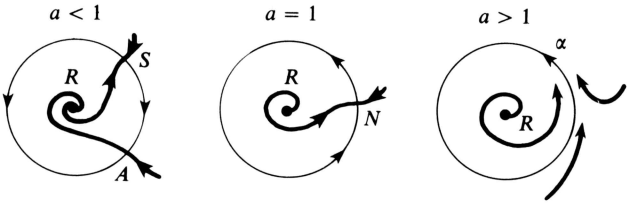

Figure 19

again stable and non-local, but we can localise it by introducing another parameter b:

$$\dot{\theta} = a - r\cos\theta$$

$$\dot{r} = br - r^3$$

This 2-parameter system is local, with organising centre at the origin; therefore the latter is a hidden organising centre for the Ω-explosion, which is given by the section $b = 1$. The bifurcation set in the parameter space consists of the line $b = 0$ of Hopf bifurcations, and the parabola $a^2 = b$ of Ω-explosions, as shown in Figure 20.

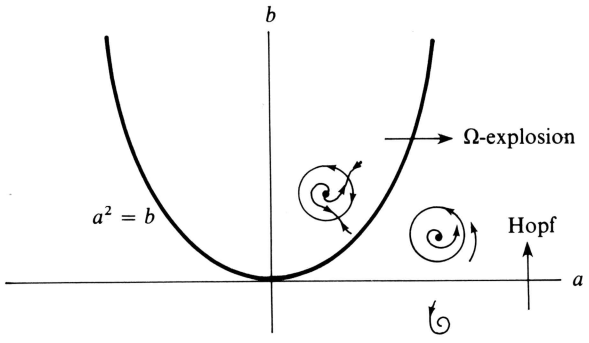

Figure 20

6.3. A Saddle Connection Catastrophe. Let the state space be $\mathbb{R}^2$, and let a be a parameter. The saddle connection is illustrated in Figure 21, and we give equations for it below, but first let us describe it qualitatively.

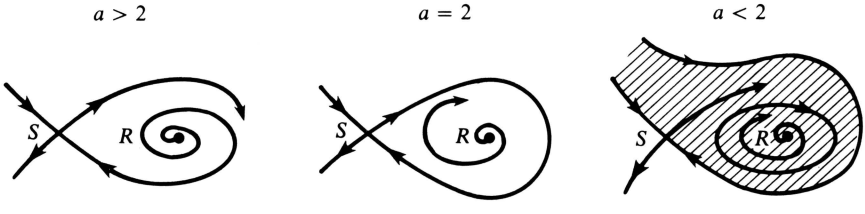

Figure 21

When $a > 2$ the nonwandering set consists of two points, a repellor R and a saddle S, and the inset of S curls inside the outset. When $a = 2$ the inset coalesces with the outset to form a saddle connection or homoclinic orbit, $\varkappa$. As a result the nonwandering set has exploded to $R \cup S \cup \varkappa$ ($\varkappa$ is nonwandering because of the orbits spiralling out from R). When $a < 2$ the inset has crossed the outset creating a new periodic attractor, α. This is a catastrophe both qualitatively and quantitatively, qualitatively because Ω_a is discontinuous at $a = 2$, and quantitatively because there is a measure-theoretic discontinuity as the new attractor captures its basin of attraction (shown shaded in Figure 21).

This example is stable and non-local, but it has a hidden organising centre at the origin of the following local 2-parameter system:

$$\dot{x} = \frac{\partial H}{\partial y}$$

$$\dot{y} = \frac{\partial H}{\partial x} + y(a - H), \quad \text{where } H = x^3 - 3bx + y^2.$$

The reader will recognise this as a parametrised damped Hamiltonian

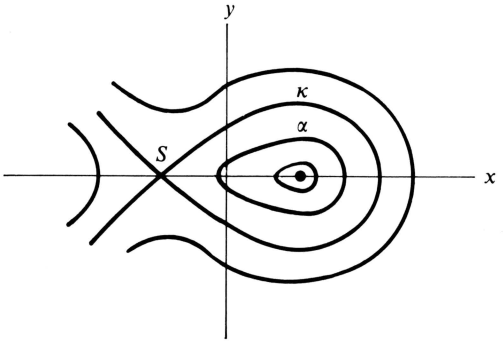

Figure 22

system [1], with Hamiltonian H and a damping that drives it to the energy level $H = a$. Figure 21 is the section given by $b = 1$. When $b = 1$ the level curves of H are shown in Figure 22; there is a minimum at $(1, 0)$ where $H = -2$, and a saddle at $(-1, 0)$ where $H = 2$. When $a \leq -2$ the minimum is an attractor of the flow, and when $a > -2$ it is a repellor; therefore when $a = 2$ there is a Hopf bifurcation at the minimum. When $-2 < a < 2$ the energy level $H = a$ contains a compact component α which is the periodic attractor shown in Figure 21. When $a = 2$ the energy level $H = 2$ contains the homoclinic orbit $\varkappa$. When $a > 2$ the energy level $H = a$ no longer contains a compact component and so the attractor disappears. Therefore $a = 2$ gives the saddle connection catastrophe, as illustrated in Figure 21.

When $b > 0$ the fixed points occur at $(\pm\sqrt{b}, 0)$ and the bifurcations occur at $a = \pm 2b\sqrt{b}$; therefore as $a, b \to 0$ the qualitative picture shrinks into the organising centre. When $a \neq 0$ and $b = 0$ the two fixed points coalesce in a fold catastrophe or saddlenode. Therefore the bifurcation set in the parameter space consists of the a-axis and the cusp $a^2 = 4b^3$, as shown in Figure 23. The negative a-axis comprises attractor-saddlenodes and the pos-

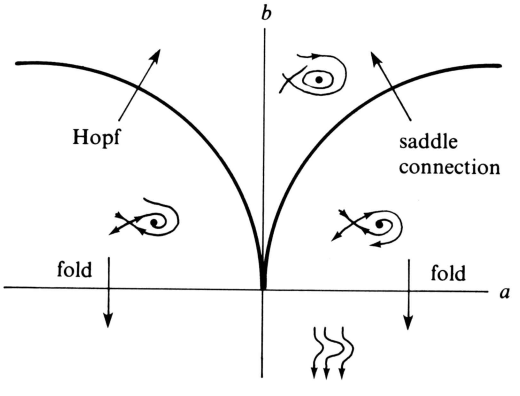

Figure 23

itive a-axis repellor-saddle-nodes; the left branch of the cusp comprises Hopf bifurcations, and the right branch saddle-connection catastrophes.

6.4. Definition of the Bowen–Ruelle Measure [9, 52, 57]. In elementary theory the phase portrait provides an adequate description of the asymptotic behaviour because the attractors are points. In the non-elementary theory, however, the phase portrait may be inadequate from the point of view of measurement because, for example, it does not provide the frequency of a periodic attractor, nor the frequency spectrum of a strange attractor. What is needed in addition to the attractor is a measure on it that describes the time spent in different parts of it, as follows. Given a flow ϕ on X, and a probability measure m on X, define the time average of m to be the measure

$$\mu = \lim_{T\to\infty} \frac{1}{T}\int_0^T \phi^t m \, dt.$$

We call μ the *Bowen–Ruelle measure.* Roughly speaking m represents the initial conditions and μ the asymptotic behaviour. For instance if the initial position is x choose m to be the Dirac measure $m = \delta_x$ with support x. If the initial position is uncertain represent this uncertainty by a suitable continuous probability measure m on X. Now for some examples of μ.

(i) If A is a point attractor and the support of m is contained in the basin of attraction of A then $\mu = \delta_A$.

(ii) If α is a periodic attractor and the support of m is contained in the basin of α then μ has support α, and at each point of α the density of μ is inversely proportional to the speed. Therefore in both these examples the Bowen–Ruelle measure exists, and is invariant, ergodic, and independent of m.

(iii) If A, B are two point attractors, and the support of m is contained in the union of their basins, and m_A, m_B are the measures of their basins, then $\mu = m_A\delta_A + m_B\delta_B$.

6.5. Parametrised Measures. Given a parametrised system, and a continuous* probability measure m, there is a time average μ_c for each parameter point c, and so we can ask the question whether or not μ_c depends continuously on c. At regular points and bifurcation points μ_c is continuous, and so it is a question of dividing the catastrophe points into those where the measure is continuous and those where it is not, as follows.

(i) At the catastrophic jump in 1.2 the measure is discontinuous because of the sudden disappearance of a basin of attraction.

(ii) At the cusp catastrophe in 1.3 the measure is continuous, but is a limit point of discontinuities.

* For parametrised systems it is better to have m continuous in order to avoid the artificial discontinuities in μ_c that arise from discontinuities in m. For example if $m = \delta_x$ and S is the separatrix between two basins, then any change in c that moves S across x will cause a jump in μ_c.

(iii) At the saddle connection catastrophe in 6.3 the measure is discontinuous because of the sudden capture of a basin of attraction. To be precise, μ_a is discontinuous as $a \searrow 2$.

(vi) At the Ω-explosion in 6.2 the measure is, surprisingly, continuous. This is the most interesting example because Ω_a is discontinuous at $a = 1$. Qualitatively it is a catastrophe, but quantitatively it behaves like a bifurcation. In an experiment one would expect to observe qualitative change, but at the same time expect quantitative time-average measurements to vary continuously. A similar phenomenon is sometimes observed at the onset of turbulence, and in the next section we shall suggest a generalisation of this example as a possible model for turbulence. Meanwhile since this is the simplest example of the phenomenon it is worth giving the proof

6.6. Lemma. *At the Ω-explosion in* 6.2 *the Bowen–Ruelle measure is continuous.*

PROOF. If $a = 1$ then, for any m, $\mu_a = \delta_N$ the Dirac measure at N. If $a < 1$ then, for any $m \neq \delta_R$, $\mu_a = \delta_A$, and so μ is continuous as $a \nearrow 1$. If $a > 1$ then μ_a is distributed over α with density $\sim (a - \cos\theta)^{-1}$, and so to prove $\mu_a \to \delta_N$ we have to show that the flow lingers longer and longer in the neighbourhood of N as $a \searrow 1$. More precisely, it suffices to show:

$$\forall \varepsilon > 0, \qquad \exists \eta > 0, \qquad \forall a,\ 1 < a < 1 + \eta \Rightarrow \mu_a[-\varepsilon, \varepsilon] > 1 - \varepsilon.$$

Let

$$A = \int_{-\varepsilon}^{\varepsilon} \frac{d\theta}{a - \cos\theta}, \qquad B = \int_{\varepsilon}^{2\pi - \varepsilon} \frac{d\theta}{a - \cos\theta}.$$

It suffices to show $B < \varepsilon A$, for then

$$\mu_a[-\varepsilon, \varepsilon] = \frac{A}{A + B} = 1 - \frac{B}{A + B} > 1 - \frac{B}{A} > 1 - \varepsilon.$$

Let $K = \int_{-\varepsilon}^{\varepsilon} (d\theta / 1 - \cos\theta)$. If $a > 1$ then $B < K$. If $a < 1 + \eta$ then

$$A > \int_{-\varepsilon}^{\varepsilon} \frac{d\theta}{(1 + \eta) - (1 - \theta^2/2)} = \frac{4}{\sqrt{2\eta}} \tan^{-1} \frac{\varepsilon}{\sqrt{2\eta}} \xrightarrow[\eta \to 0]{} \infty.$$

If η is sufficiently small then $A > K/\varepsilon$. Therefore, $B < K < \varepsilon A$, as required. This completes the proof that μ_a is continuous at $a = 1$. □

7. Strange Attractors

In this section we define and construct some strange attractors. We give both a topological definition 7.1 and a measure theoretic definition 7.8. The strange attractors that are best understood are those that satisfy axiom A

(see 7.6), but models of turbulence are more likely to need non-axiom A attractors (see 7.9). In particular the onset of turbulence would be modelled by a strange bifurcation, and in 7.11 we describe an example in which a periodic attractor runs into a strange saddle causing an Ω-explosion into a strange attractor. For further examples of strange attractors see [4, 7, 8, 20, 23, 24, 28, 29, 34, 38, 42, 45, 50, 55, 60, 61, 64, 66, 74, 75].

7.1. Topological Definition of Attractor. An *attractor* Λ of a flow ϕ on X is a subset that is attracting and indecomposable. Here *attracting* means $\exists$ a closed positively-invariant* neighbourhood N of Λ such that $\bigcap_{t>0} \phi^t N = \Lambda$. *Indecomposable* means $\exists$ a point in Λ whose ω-limit* is Λ.

It follows that Λ is a closed invariant subset of the nonwandering set Ω. One can also deduce that Λ is minimal in the sense that if one attractor contains another, or if two meet, then they are equal. Define the *basin of attraction* of Λ to be the set of points whose ω-limit is contained in Λ; it follows that the basin is an open invariant set containing N. Call Λ *stable* if perturbations of ϕ have an equivalent attractor nearby.

7.2. Examples. There are three types of *familiar* attractors, and all the rest are called *strange* attractors (because they have only really been studied in the last 20 years or so). The familiar attractors are:

(i) *Point Attractor.* A point attractor is stable if hyperbolic; here hyperbolic means the eigenvalues have non-zero (and hence negative) real part.

(ii) *Periodic Attractor.* Here the attractor is diffeomorphic to the circle $T = \mathbb{R}/\mathbb{Z}$, and is stable if hyperbolic.

(iii) *Quasi-periodic Attractor.* Here the attractor is diffeomorphic to an n-torus, $T^n = \mathbb{R}^n/\mathbb{Z}^n$, $n \geq 2$, and the flow is equivalent to an irrational flow, given by $\phi^t x = x + \omega t$, where $\omega = (\omega_1, \ldots, \omega_n)$ is constant and the ω_i are irrationally related. Therefore all orbits are dense. A quasi-periodic attractor is unstable because any rational perturbation has all orbits periodic. Moreover, if we perturb further by adding a suitable small transverse field then we obtain a stable flow with a single periodic attractor L, whose basin is dense in T^n. Such an L is called a *lock-on* because it locks all the phases of the original n oscillators together; the collapse of the attractor $T^n \to L$ is called an Ω-*implosion.*

Before we go on to construct a strange attractor we make a remark about definition 7.1 above.

Remark. There is no universally accepted definition of attractor yet because the subject is still developing. Most definitions are either too strong because they exclude important examples, or too weak because they include un-

* *Positively-invariant* means $\phi^t N \subset N$, $\forall t > 0$. The ω-*limit* of x means $\bigcap_t$ (closure $\bigcup_{s>t} \phi^s x$).

wanted examples. For instance, that in [72, page 39] is slightly too strong because it inadvertently excludes strange attractors; that in [64, page 786] is only concerned with axiom A and excludes non-axiom A attractors; that in [1, page 517] is slightly too weak because it lacks minimality, and includes, for example, all closed invariant sets of the equation $\dot{x} = -x$ on $\mathbb{R}^n$. The definition above may need to be weakened when studying strange bifurcations. Also some authors prefer a more measure-theoretic definition, like 7.8 below, because it is more closely related to the measurements made in experiments. On the other hand, it is important to keep both the topological and the measure-theoretic viewpoints in mind because the former provides an overall grasp, while the latter relates to data.

We shall now construct a strange attractor by suspending a diffeomorphism. This is the simplest method of constructing one, and indeed the study of diffeomorphisms was pioneered by Smale [64] in order to gain insight into differential equations. The most elegant attractors are obtained from Anosov diffeomorphisms [4, 30, 64], but these are exceptional because they are manifolds and do not display the Cantor set structure that is typical of most strange attractors; so instead we shall describe some examples that are more likely to be of use in modelling turbulence.

7.3. Definition of Suspension. Given a smooth embedding $f\colon M \to M$ we suspend this to a flow Σf on a manifold $\Sigma_f M$ one dimension higher, as follows. Let $F\colon \mathbb{R} \times M \to \mathbb{R} \times M$ be the map $F(s, x) = (s - 1, fx)$ and define $\Sigma_f M$ to be the quotient manifold $(\mathbb{R} \times M)/F$. Let ϕ be the flow on $\mathbb{R} \times M$ given by $\phi^t(s, x) = (s + \omega t, x)$, where $\omega > 0$. We call ω the *frequency* of the suspension. Since ϕ commutes with F it induces a flow on $\Sigma_f M$, which defines Σ_f.

If f is a diffeomorphism there is a simpler way of constructing $\Sigma_f M$ by glueing the ends of $I \times M$ together with f, so that $(1, x) = (0, fx)$ (see Figure 24).

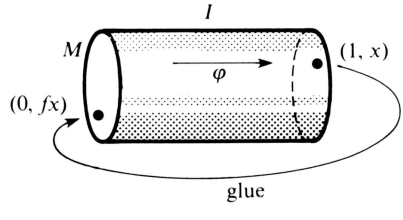

Figure 24

The fixed points and (discrete) periodic orbits of f suspend into the (continuous) periodic orbits of Σf. The attractors of f suspend into the attractors of Σf. Here an attractor of an embedding is defined in the same way, word for word, as an attractor of a flow (with the understanding in 7.1 that t lies in $\mathbb{Z}$ rather than $\mathbb{R}$).

7.4. Example of a Strange Attractor [61, 64]. Let M be the 3-dimensional solid torus

$$M = \{(w, z);\ w, z \in \mathbb{C},\ |w| = 1,\ |z| \leq 1\}.$$

Define the embedding $f\colon M \to M$ by

$$f(w, z) = \left(w^2,\ \frac{w}{2} + \frac{z}{4}\right).$$

Let

$$\Lambda = \bigcap_{n>0} f^n M$$

(see Figure 25). We shall show that Λ is a strange attractor of f. Therefore if we suspend f to give a flow Σ_f on the 4-dimensional manifold $\Sigma_f M$, then $\Sigma\Lambda$ will be a strange attractor of the flow.

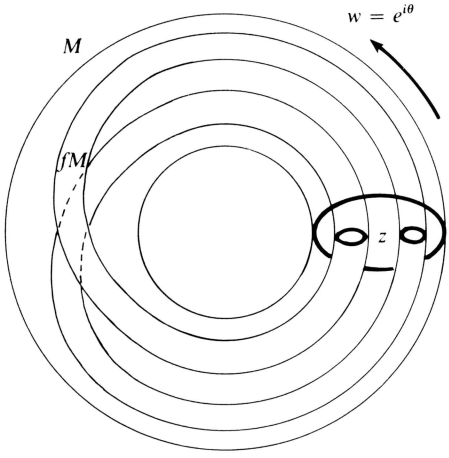

Figure 25

Before proving Λ is an attractor, let us describe its geometry. The image fM of f is a long thin torus that winds twice round inside M, and meets each transverse disk $w =$ constant in 2 small disks, each of radius $\frac{1}{4}$. Similarly f^2M is a longer thinner torus that winds 4 times round, and meets each disk in 4 small disks, each of radius $\frac{1}{16}$, and so on. In the limit Λ meets each disk in a Cantor set. Therefore locally Λ is the 1-dimensional product of an arc and a Cantor set, and globally Λ is a bundle over the circle with fibre the Cantor set (like a solenoid). Consequently the suspension $\Sigma\Lambda$ is locally the 2-dimensional product of a surface and a Cantor set.

7.5. Lemma. *Λ is a stable attractor of f.*

PROOF. By construction Λ is attracting, and so it suffices to prove it indecomposable. Following Parry we prove Λ indecomposable by showing $f \mid \Lambda$

conjugate to a shift automorphism, as follows. Let $2^{\mathbb{Z}}$ denote the space of all doubly-infinite sequences of 0's and 1's, with the compact-open topology. Let σ be the left-shift on $2^{\mathbb{Z}}$ given by $(\sigma y)n = y(n+1)$, $y \in 2^{\mathbb{Z}}$, $n \in \mathbb{Z}$. Given

$$x = (e^{i\theta}, z) \in \Lambda \quad \text{let } h_0 x = \begin{cases} 0, & 0 \le \theta < \pi \\ 1, & \pi \le \theta < 2\pi. \end{cases}$$

Applying h_0 to the orbit $[\ldots, f^{-1}x, x, fx, f^2x, \ldots\}$ of x determines a map $h\colon \Lambda \to 2^{\mathbb{Z}}$, which is not continuous, but which makes the following diagram commutative:

$$\begin{array}{ccc} \Lambda & \xrightarrow{f} & \Lambda \\ {\scriptstyle h}\downarrow & & \downarrow{\scriptstyle h} \\ 2^{\mathbb{Z}} & \xrightarrow{\sigma} & 2^{\mathbb{Z}} \end{array}$$

Now $h\Lambda$ consists of all sequences except those ending in an infinite string of 1's. Therefore, as in decimals, let us identify a sequence ending 0111... with the sequence having the same beginning but ending 1000..., and identify the sequence of all 1's with that of all 0's. Let Λ^* be the identification space, and $v\colon 2^{\mathbb{Z}} \to \Lambda^*$ the identification map. It is straightforward to verify that although h is not continuous the composition $vh\colon \Lambda \to \Lambda^*$ is in fact a homeomorphism. Therefore $f \mid \Lambda$ is conjugate to the left-shift on Λ^*. The periodic orbits in $h\Lambda$ are dense in $2^{\mathbb{Z}}$, and hence it is easy to construct a point in $h\Lambda$ with ω-limit $2^{\mathbb{Z}}$. Therefore periodic orbits are dense in Λ^*, and Λ^* is indecomposable. Therefore the same is true for Λ, and so Λ is an attractor. For the proof of stability the reader is referred to [39, 44, 65]. □

7.6. Definition of Axiom *A* Attractor. Following Smale [64] we say an attractor Λ of a flow on X satisfies *axiom A* if periodic orbits are dense in Λ and Λ has a hyperbolic structure; here a *hyperbolic structure* means that at each point Λ there is

$$\begin{cases} 1 \text{ dimension of flow} \\ e \text{ dimensions of expansion} \\ n - 1 - e \text{ dimensions of contraction} \quad (n = \dim X), \end{cases}$$

and that this decomposition is continuous (see [30, 64] for details). For instance example 7.4 above satisfies axiom A: the periodic orbits are dense by the lemma, and it is hyperbolic because there is 1 dimension of flow in the suspension direction, 1 dimension of expansion in the w-direction, and 2 dimensions of contraction in the z-direction. Locally an axiom A attractor is always like a manifold in the flow and expansion directions, but may be like a submanifold, or a Cantor set, of a product of the two, in the contraction direction.

In a familiar attractor there is no expansion and so $e = 0$, but in a strange attractor these must always be an expanding direction, and so $e \ge 1$. This

expanding quality is an extremely important property of strange attractors because points that are close together are torn apart exponentially. Therefore it implies *sensitive dependence on initial condition* [54], and gives an unpredictable and chaotic appearance to the motion [28, 50, 55, 60]. At the same time the advantage of axiom A is that it is a sufficient condition for the attractor to be stable [39, 65]. Hence we have that paradoxical combination of chaos and stability which is so noticeable in turbulence. Axiom A attractors also have nice measure theoretical properties, as follows. Recall the Definition 6.4 of the Bowen–Ruelle measure.

7.7. Theorem (Bowen–Ruelle [9, 52]). *If Λ is an axiom A attractor with basic B then for any continuous probability measure m with support in B the Bowen–Ruelle measure μ exists, has support Λ, and is invariant, ergodic, and independent of m.*

Remark. If an attractor Λ is strange there must be some exceptional points in its basin B whose ω-limit is not the whole of Λ; for instance each periodic orbit inside Λ must be the ω-limit of some exceptional points. If x is exceptional the time average of δ_x cannot equal the Bowen–Ruelle measure μ on Λ—that is why we required m to be continuous in Theorem 7.7. However, if Λ satisfies axiom A these exceptional points only have Lebesgue measure zero. Therefore the complementary set B_0 of generic points has Lebesgue measure 1 in B, and $\forall x \in B_0$, $\mu =$ the time average of δ_x. In other words, most initial conditions lead to μ.

Now suppose $g\colon B \to \mathbb{R}$ is a continuous function representing some experimental measurement. Define the time average $\bar{g}$ of g to be

$$\bar{g}x = \lim_{T\to\infty} \frac{1}{T}\int_0^T g(\phi^t x)\, dt.$$

Then Theorem 7.7 implies that $\bar{g}$ is constant on B_0 and

$$\bar{g}x = \int_\Lambda g\, d\mu, \qquad \forall x \in B_0.$$

The significance of this result is that in spite of sensitive dependence on initial condition, the time-average measurements are not sensitive. Although the flow may look chaotic the measurements are meaningful and repeatable. Rand [47] suggests that since this property of attractors is the most important one from the experimental point of view it ought to be embodied in the definition, in order to distinguish those attractors that might be useful for modelling. He therefore proposes that the following definition might be a fruitful extension of axiom A.

7.8. Measure-Theoretic Definition of Attractor. Given a flow ϕ on X and an open set $B \subset X$ we say *there is an attractor in B* if the time average of any function B is almost constant. Here *almost constant* means $\exists$ a subset B_0, of

Lebesgue measure 1 in B, such that, $\forall$ continuous $g: B \to \mathbb{R}$, $\bar{g}$ is constant on B_0. It follows that the Bowen–Ruelle measure μ exists, and, $\forall g$, $\bar{g} = \int g \, d\mu$. The *attractor* Λ is defined to be the support of μ.

7.9. The Henon Attractor [23]. Non-axiom A attractors are relatively unexplored but are the subject of much current research. The best known examples are the Lorenz attractor [20, 28, 45, 53, 75] and the Henon attractor, although neither of these has been proved to satisfy either of the above definitions yet.

The Henon attractor is a closed invariant set Λ of the diffeomorphism $f: \mathbb{R}^2 \to \mathbb{R}^2$ given by $f(x, y) = (y + 1 - ax^2, bx)$, where $a = 1.4$, $b = 0.3$. Henon [23] proved that Λ is attracting, and used a computer to show it looks like Figure 26. However Λ has not yet been proved indecomposable,

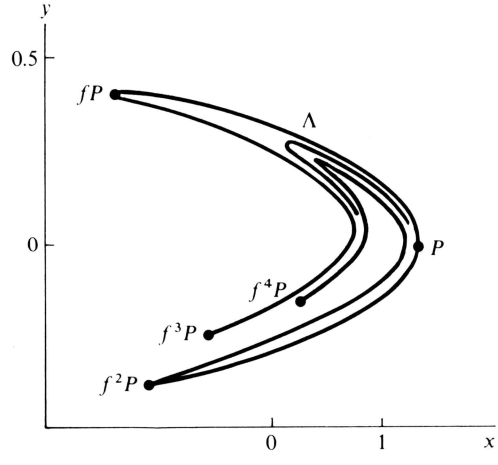

Figure 26

although numerical results suggest that it is. The computer pictures look as if Λ is locally the product of an arc and a Cantor set, but this is unlikely to be true for the following reason. If $P \in \Lambda$ is a point on the x-axis, then it can be seen from Figure 26 that the arc through P gets folded sharper and sharper under the iterations of f, so that, if the images of P are dense in Λ, then any open subset of Λ must contain an infinity of them and cannot therefore be a product. This phenomenon also prevents Λ from being hyperbolic. Therefore it does not satisfy axiom A and is difficult to handle with Smale theory; however, it may be possible to show it is a measure-theoretic attractor in the sense of 7.8 by using characteristic exponents and the more general Pesin theory [41, 56]. For some values of the parameters (a, b) computer studies suggest that Λ breaks up into a (possible infinite [37]) number of periodic attractors. Even if this were to happen for a dense set of parameters nevertheless it may be possible to estimate a bound for the variation of the

associated Bowen–Ruelle measure μ, which is really what is needed from the experimental point of view.

Meanwhile Lozi [29] has studied the piecewise-linear analogue of the Henon attractor, given by replacing x^2 by $|x|$ in the definition of f, and Misiurewicz [34] has shown it indecomposable for an open set V of parameters. Although the Lozi attractor is not smooth it does satisfy Definition 7.1, and probably the associated Bowen–Ruelle measure is continuous in V.

The map f in the Henon attractor is orientation reversing, but an orientation preserving analogue is obtained by changing the sign of b, and then the suspension Σf gives a 2-dimensional strange attractor in a 3-dimensional solid torus, which is much closer to the type of attractor we are looking for to model turbulence.

7.10. The Horseshoe [62, 63, 64]. If we are to model the onset of turbulence by a strange bifurcation, it is necessary to study strange saddles as well as strange attractors. The most famous strange saddle is the Smale horseshoe, which is defined as follows.

Let M be the union of a square Q and two semi-disks D, D'. Let $f\colon M \to M$ be a horseshoe-shaped embedding, as shown in Figure 27, such that on the

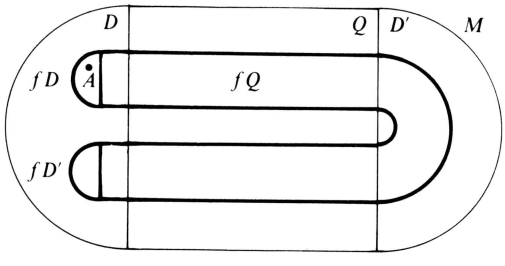

Figure 27

semi-disks f is contracting, and on $f^{-1}Q \cap Q$ it is linear and hyperbolic, expanding horizontally and contracting vertically. Then there is a unique point attractor $A \in fD$, and the rest of the nonwandering set is the strange saddle H, defined as follows.

Let $Q_0 = Q$, let $Q_{n+1} = f^{-1}Q_n \cap fQ_n$ inductively, and let $H = \bigcap_n Q_n$. Then Q_1 comprises 4 small rectangles, Q_2 comprises 16 smaller rectangles, and so on, until in the limit H is the product of two Cantor sets, and hence is itself a Cantor set (see Figure 28). H is invariant, indecomposable and densely filled with periodic points, because $f|H$ is conjugate to the left-shift on $2^{\mathbb{Z}}$ (as in Lemma 7.5). H is hyperbolic by construction, and so satisfies axiom A. Therefore H is a strange saddle, and stable [63].

In particular H contains two fixed points S, S' which are both saddle points. S is the top left corner of H and S' is near the bottom right corner. Let $\Lambda = \bigcap_{n>0} f^n M$, as shown in Figure 29. In fact Λ is the union of the sink A and the outset of H. Locally Λ is the product of an arc and a Cantor set,

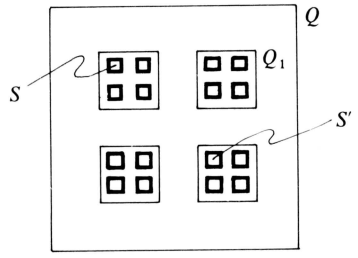

Figure 28

except at A. Notice that Λ is attracting but it is not an attractor because it is not indecomposable. In fact the points of $\Lambda - H - A$ are wandering, and wander off to A. The outsets of S, S' are contained in Λ; the left outset of S is the interval SA running straight into A, while the right outset of S and both outsets of S' wind densely over Λ.

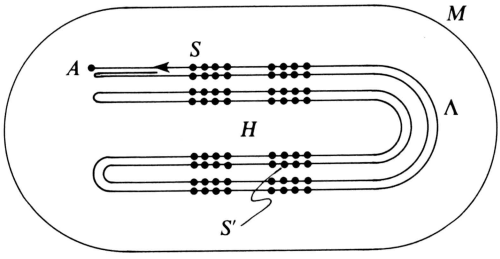

Figure 29

7.11. The Sink-Horseshoe Bifurcation. This is an example of a strange bifurcation which might be useful in modelling, but which is not yet fully understood mathematically and needs to be studied further. Introduce a parameter in the above construction of the horseshoe, and use the parameter to change f in the neighbourhood of AS so as to run the sink A into the saddle point S. Locally this is the simplest form of catastrophe, namely a saddlenode or fold catastrophe, but globally we must regard it as a sink running into the strange saddle H, because H is indecomposable. It is analogous to the Ω-explosion of Example 6.2, because the nonwandering set explodes* from $A \cup H$ into Λ. Roughly speaking after the bifurcation all the

* More precisely, let c be the parameter, $c = 0$ the bifurcation point, Ω_c the nonwandering set of f_c, $\Omega = \bigcup c \times \Omega_c$, $\bar{\Omega} =$ closure Ω, $\bar{\Omega}_c = \bar{\Omega} \cap (c \times M)$, and $\Lambda_c = \bigcap_n f_c^n M$. Then

$$\Omega_c = \bar{\Omega}_c = A_c \cup H_c, \qquad c > 0$$

$$\Omega_0 = H_0$$

$$\bar{\Omega}_0 = \Lambda_0 .$$

We know $\Omega_c \subset \Lambda_c$, $\forall c$, and $\Omega_c \neq \Lambda_c$ for some positive values of c near 0, but conjecture that $\Omega_c = \Lambda_c$ for some other positive values of c near 0.

points of Λ which used to wander off to A now re-enter again at S and go round Λ again. After the bifurcation S has disappeared and so an exponentially thin neighbourhood of the outset of S has been removed from Λ, but S' is preserved, and Λ is probably still the closure of its outset. In fact Λ resembles the Henon attractor 7.9 (with $b < 0$). For all parameter values Λ is attracting but for some values after bifurcation it cannot be an attractor, because it contains periodic sinks with very long periods and very small basins [37], and is therefore not indecomposable. However we conjecture* that the Bowen–Ruelle measure is continuous at the bifurcation point, as in Lemma 6.6.

Suppose that we now suspend the whole picture to give a parametrised flow Σ_f on the 3-dimensional open solid torus $\Sigma_f M$. Before bifurcation ΣA is a periodic attractor in the torus representing periodic motion, and after bifurcation $\Sigma\Lambda$ is (or, more precisely, resembles) a 2-dimensional strange attractor representing turbulence. At bifurcation the Ω-explosion represents the qualitative catastrophic onset of turbulence, and the μ-continuity represents the quantitative continuity of time-average measurements. We pursue this model further in 8.4 below.

8. Turbulence

Ruelle and Takens [51] first proposed the use of strange attractors to model turbulence in 1971. This intriguing idea has attracted a great deal of attention, but as yet the programme is still in its infancy: much of the mathematics is still unresolved, and the application is mostly speculative. The future mathematical programme will require:

(i) topological studies of strange bifurcations and their organising centres (extending the ideas of Sections 5 and 6);
(ii) measure theoretic studies of strange bifurcations, generalising Fourier analysis from periodic attractors to strange attractors;
(iii) quantitative analysis of the Navier–Stokes equations at the strange organising centres (as in Section 4), leading to prediction and experimental confirmation.

The central idea of the programme is to provide a conceptually simple geometric link between the complexity of the Navier–Stokes equations on the one hand and the complexity of the observed data on the other. In this section we discuss some points in the programme. For further discussions see [7, 8, 12, 13, 14, 26, 28, 35, 47, 50, 53, 54, 55, 57, 60, 66, 67, 70].

8.1. The Ruelle–Takens Model. We begin with the Landau–Lifschitz model [26] for the onset of turbulence. Let X be the space of all possible fluid

* This conjecture is the reason for calling it a bifurcation rather than a catastrophe.

velocity fields in a given region, and let E be the evolution equation on X determined by the Navier–Stokes equations and parametrised by the Reynold's number R. For $R < R_1$ suppose that E has a point attractor T^0, representing steady fluid motion. At R_1 there is a Hopf bifurcation $T^0 \to T^1$, to a periodic attractor T^1 representing periodic fluid motion. If the Reynolds number is increased to R_2 there is another Hopf bifurcation $T^1 \to T^2$, to a quasi-periodic attractor on a torus T^2 (see 7.2). At R_3 here is further Hopf bifurcation $T^2 \to T^3$, to a quasi-periodic attractor on a 3-dimensional torus T^3, and so on, giving the sequence of bifurcations

$$T^0 \to T^1 \to T^2 \to T^3 \to \cdots$$

as the Reynolds number increases, leading eventually to turbulence.

Ruelle and Takens criticised the Landau–Lifschitz model on the grounds that since T^n is unstable for $n \geq 2$ it is unlikely to be observed. They showed [38, 51] that for $n \geq 3$ there exist stable perturbations $T^n \to \Lambda$, where Λ is a strange attractor in T^n of lower dimension. Then the strange attractor will exhibit the desired sensitive dependence on initial condition [54]. Although this was a far reaching idea, the Ruelle–Takens model can itself be criticised on three grounds, as follows.

(i) Applying their own criticism and construction to the case $n = 2$ gives a lock-on $T^2 \to L$, where L is a periodic attractor (see 7.2). This modifies the Landau–Lifschitz sequence to $T^0 \to T^1 \to T^2 \to L$, so that we never actually reach the situation T^n, $n \geq 3$, where the Ruelle–Takens construction can be used to obtain a strange attractor.

(ii) The particular examples [42] of strange attractors that they used to prove the mathematical existence theorem are not particularly plausible from the hydrodynamic point of view (not that they claimed any such plausibility).

(iii) At the onset of turbulence new fluid motions appear that were not observed before turbulence, and so this suggests an Ω-explosion rather than an Ω-implosion $T^n \to \Lambda$.

8.2. Experimental Data. The most interesting data obtained so far are that of Gollub, Swinney and their collaborators [12, 13, 14, 67]. They measured frequency spectra in Bénard and Taylor flows, and inferred that the following are amongst typical routes to turbulence:

$$\text{Bénard:} \quad T^0 \to T^1 \to T^2 \to L \to \text{turbulence}$$

$$\text{Taylor:} \quad T^0 \to T^1 \to T^2 \to \text{turbulence.}$$

The Bénard experiment [14] consists of heating a rectangular cell of water from below, the parameter in this case being the Rayleigh number or temperature difference. Firstly, there is a steady motion T^0, consisting of rolls parallel to the longer side, as shown in Figure 30. Secondly, when the temperature is increased the rolls begin to oscillate to and fro with a frequency

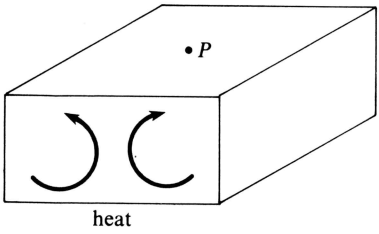

Figure 30

ω_1, say, which is represented by a bifurcation $T^0 \to T^1$ to a periodic attractor. Thirdly, the amplitude of the oscillations begins to modulate with frequency ω_2, say, which is represented by a bifurcation $T^1 \to T^2$ to a quasi-periodic attractor. Fourthly, there is a phase lock between oscillations and modulation $T^2 \to L$, both the original frequencies now being multiples of the lock-on frequency ω. Fifthly, the onset of turbulence is accompanied by a broadening of the spectral lines to bands. A typical sequence of frequency spectra is sketched in Figure 31. [See 12, 14.]

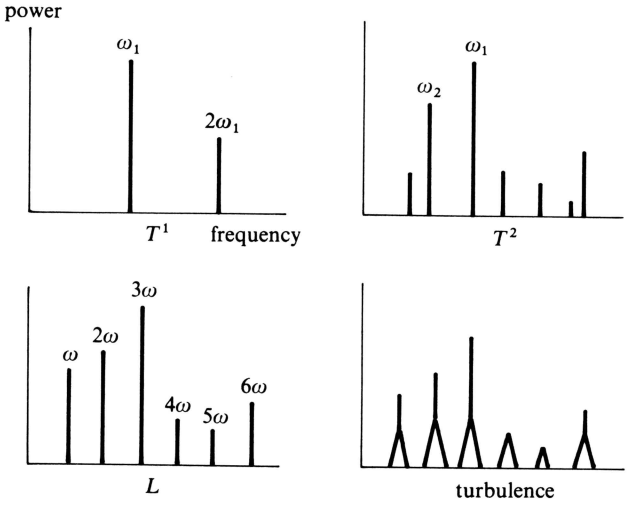

Figure 31

These spectra are obtained by monitoring some component v of the fluid velocity at a suitable point, for instance the horizontal component at P in Figure 30. The velocity is calculated from the Doppler effect on a laser beam focused at P and reflected off tiny polystyrene balls moving with the fluid. Then the spectrum is the Fourier transform of the autocorrelation function of v (see 8.3 below).

In the Couette–Taylor experiment T^0 represents the steady motion of Taylor flow described in Section 4, above. When the Reynolds number is

increased the Taylor cells develop waves which rotate at (mysteriously) one third the angular velocity of the inner cylinder, which is represented by a bifurcation $T^0 \to T^1$ to a periodic attractor. Next the amplitude of the waves begins to modulate, which is represented by $T^1 \to T^2$. Finally the onset of turbulence is accompanied by a broadening of the spectral lines. There is no lock-on in this case because T^2 is stable with respect to the rotational symmetry of the apparatus [18, 46]. We now have to explain why a strange bifurcation causes a broadening of the spectral lines.

8.3. Fourier Analysis. Let ϕ be a flow on X and $v\colon X \to \mathbb{R}$ a measurement. If the initial condition is $x \in X$ then the autocorrelation function $\alpha\colon \mathbb{R} \to \mathbb{R}$ of v is defined by

$$\alpha(t) = \lim_{T\to\infty} \frac{1}{T}\int_0^T v(\phi^s x)v(\phi^{s+t}x)\,ds.$$

Assuming x is a generic initial condition in the basin of an attractor Λ with Bowen–Ruelle measure μ, then

$$\alpha(t) = \lim_{T\to\infty} \frac{1}{T}\int_0^T g^t(\phi^s x)\,ds, \quad \text{putting } g^t(x) = v(x)v(\phi^t x),$$

$$= \int_\Lambda g^t\,d\mu, \quad \text{which is independent of } x.$$

The frequency spectrum σ is the Fourier transform of α, and we now describe some examples.

(i) If $\Lambda = T^1$, a periodic attractor of frequency ω, then

$$\sigma = \sum_{n=1}^{\infty} \sigma_n \delta_{n\omega},$$

where $\delta_{n\omega}$ is the Dirac measure at $n\omega$ and σ_n the energy in the nth harmonic. Therefore the spectrum consists of lines at the multiples of ω, with heights σ_n, as in the first and third graphs of Figure 31. If we change the measurement v this merely alters the heights of the spectral lines. If ϕ depends upon a parameter like the Reynolds number, and we perturb the parameter, then this may move Λ in X and alter the fundamental frequency ω; it may also alter the speed with which ϕ flows round Λ differently in different parts of Λ, and hence change the harmonics, in other words, alter the heights of the spectral lines, but it will not change the type of σ.

(ii) If $\Lambda = T^2$, a quasi-periodic attractor with frequencies ω_1 and ω_2, then

$$\sigma = \sum_{n_1, n_2} \sigma_{n_1, n_2} \delta_{n_1\omega_1 + n_2\omega_2}$$

as in the second graph of Figure 31. Changing the measurement may alter the heights of the spectral lines, and perturbing the parameter may

alter their heights and change the fundamental frequencies ω_1 and ω_2, but as long as Λ remains quasi-periodic it will not change the type of σ. This is particularly noticeable in modulated wavy Taylor flow because the symmetry makes T^2 stable [18, 46].

(iii) If the attractor is a suspension $\Sigma\Lambda$ of frequency ω, and if the measurement v depends only on the suspension coordinate, then σ will be the same as in case (i), giving the appearance of a periodic attractor. If, however, $\Sigma\Lambda$ is in fact a strange attractor, and if a perturbation of the parameter causes the speed to alter differently in different parts of $\Sigma\Lambda$ then this will uniformly broaden each spectral line into a band, as in Figure 31, because the expanding property of the strange attractor causes mixing and destroys the correlation after some time [40, 47]. For example if the change of speed caused an ε-change in the suspension frequency that depended linearly on Λ then this would destroy the correlation after time $\sim (1/\varepsilon)$, and hence broaden each spectral line into a band of width $\sim \varepsilon$. The greater the change of speed the broader the bands, until they eventually overlap and lose their identity.

8.4. Onset of Turbulence. We return to the main problem of finding bifurcations that model the onset of turbulence. Suppose that turbulence is preceded by periodic motion, represented by a periodic attractor T^1 of the evolution equation E on X. Let M be a disk of codimension 1 in X, cutting T^1 transversally at A, say. Let f: $M \to M$ be the Poincaré return map determined by E. Then A is a point attractor of f, and its suspension $\Sigma A = T^1$. Assume that A is stable, so that all its eigenvalues have negative real part.

In the Landau–Lifschitz model the next step $T^1 \to T^2$ is equivalent to assuming a Hopf bifurcation of f at A, which is preceded by the weakening of the attractive power of a pair of complex eigenvalues just before they cross the imaginary axis. An alternative assumption is the weakening of a single real eigenvalue. This is particularly plausible in the case when T^1 has arisen from a lock-on $T^2 \to T^1$, because then the eigenvalue of T^1 in T^2 is already weak compared with the rest.

When a real eigenvalue crosses the imaginary axis from negative to positive it produces a pitchfork bifurcation of f, as in Figure 1. (Here the equilibrium set for the parametrised embedding is equivalent to that for the parametrised flow in 1.1.) Now the pitchfork is unstable, so we look for a bifurcation arising from a stable perturbation of the pitchfork. In elementary theory the only stable perturbation of the pitchfork that contains any bifurcations or catastrophes on its primary branch is that shown in the middle picture of Figure 14; here the attractor A runs into a saddle causing a catastrophic jump to another attractor. In non-elementary theory we must allow for the possibility that the saddle might be strange, in which case we should obtain an Ω-explosion similar to the sink-horseshoe bifurcation 7.11. Indeed this example is not implausible as we now explain.

Given a weak real eigenvalue, the Poincaré return map can be written as

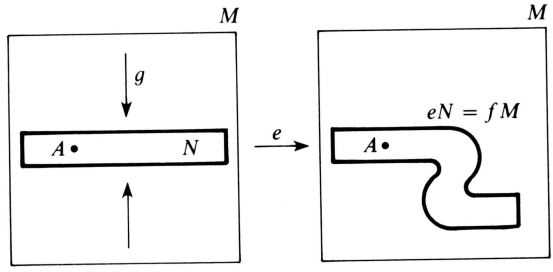

Figure 32

a composition $f = eg$, where g is a strong contraction onto a tubular neighbourhood N of the corresponding eigenvector, and e is an embedding of N in M. Locally near A the embedding maps N along the eigenvector, but globally e may bend N, as in Figure 32. Indeed the return map of a Hopf bifurcation has a similar S-bend, except that in the Hopf case A lies in the middle of the S-bend. Therefore Figure 32 could be regarded as a perturbation of the Landau–Lifschitz model, and it would be interesting to find a common organising centre.

It is possible to obtain Figure 32 by extending Figure 27, and in this case the nonwandering set of f will be the attractor A and a horseshoe as in 7.10. Then the required perturbation of the pitchfork will be none other than the sink-horseshoe bifurcation $A \to \Lambda$ described in 7.11. The suspension $\Sigma A \to \Sigma\Lambda$ is an Ω-explosion from the periodic attractor T^1 to the strange attractor $\Sigma\Lambda$ modelling the onset of turbulence.

Now in an experiment the experimenter will naturally set up his apparatus so as to best detect T^1 and measure its frequency before bifurcation. Therefore immediately after bifurcation the apparatus will automatically pick up the suspension coordinate of $\Sigma\Lambda$, and measure its frequency. Hence, assuming the Bowen–Ruelle measure continuous at bifurcation, the spectral lines will exhibit no discontinuity at the Ω-explosion. Beyond bifurcation the speed of $\Sigma\Lambda$ will begin to depend on Λ as well as on the suspension coordinate, and so the spectral lines will begin to broaden uniformly into bands.

In the case of Taylor flow the rotational symmetry of the apparatus will induce a double suspension $\Sigma^2 A \to \Sigma^2\Lambda$. Therefore the quasi-periodic torus T^2 explodes into a 3-dimensional strange attractor, accompanied by a broadening of the quasi-periodic spectral lines.

8.5. Summary. Strange bifurcations involving Ω-explosions from periodic attractors to strange attractors have properties that resemble the onset of turbulence, as follows:

(i) catastrophic qualitative change;
(ii) continuous quantitative change;
(iii) expanding properties, implying sensitive dependence on initial condition, and chaotic appearance;

(iv) indecomposable properties, implying that time-average measurements are independent of initial condition;
(v) mixing properties, implying the uniform broadening of frequency spectral lines into bands;
(vi) stability properties, implying the stability of turbulent flow, and the repeatability of measurements.

It should be emphasised, however, that much of the mathematics is incomplete as yet, and still developing.

References

1. R. Abraham and J. E. Marsden, *Foundations of mechanics* (2nd edition), Benjamin, Reading, MA 1978.
2. R. Abraham and S. Smale, Nongenericity of Ω-stability, *Global Analysis, Proc. Symp. Pure Math. Vol. 14*, Am. Math. Soc., Providence, RI, 1970, 5–8.
3. A. Andronov and L. Pontryagin, Systèmes grossiers, *C.R. (Dokl.) Acad. URSS* **14** (1937), 247–251.
4. D. V. Anosov, Geodesic flows on closed Riemannian manifolds with negative curvature, *Proc. Steklov Inst. Math.* **90** (1967), 1–235.
5. V. I. Arnold, Criticial points of smooth functions and their normal forms, *Russian Math. Surveys* **30** (1975), 1–75.
6. T. B. Benjamin, Bifurcation phenomena in steady flows of a viscous fluid, in *Proc. Roy. Soc. Lond. A* **359** (1978), 1–43.
7. P. Bernard and T. Ratiu (Eds.), *Turbulence Seminar*, Lecture Notes in Math. Vol. 615, Springer-Verlag, Berlin, 1977.
8. R. Bowen, A model for Couette flow data, *Turbulence Seminar*, Lecture Notes in Math. Vo. 615, Springer-Verlag, Berlin, 1977, 117–133.
9. R. Bowen and D. Ruelle, The ergodic theory of Axiom *A* flows, *Inventiones Math.* **29** (1975), 181–202.
10. J. J. Callahan, Special bifurcations of the double cusp, Preprint, Smith College, Northampton, MA 1978.
11. M. M. Couette, Études sur le frottement des liquides, *Ann. Chim. Phys.* **6**, Ser. 21 (1890), 433–510.
12. P. R. Fenstermacher, H. L. Swinney, and J. P. Gollub, Dynamical instabilities and the transition to chaotic Taylor vortex flow, *J. Fluid Mech.* **94** (1979), 103–128.
13. J. Gollub and H. L. Swinney, Onset of turbulence in a rotating fluid, *Phys. Rev. Lett.* **35** (1975), 927–930.
14. J. P. Gollub and S. V. Benson, Many routes to turbulent convection, *J. Fluid Mech.* **100** (1980), 449–470.
15. M. Golubitsky, An introduction to catastrophe theory and its applications, *SIAM Rev.* **20** (1978), 352–387.
16. M. Golubitsky and D. Schaeffer, A theory for imperfect bifurcation via singularity theory, *Commun. Pure and Appl. Math.* **32** (1979), 21–98.
17. M. Golubitsky and D. Schaeffer, Imperfect bifurcation in the presence of symmetry, *Commun. Math. Phys.* **67** (1979), 205–232.
18. M. Gorman, H. L. Swinney, and D. Rand, Quasi-periodic circular Couette flow: Experiments and predictions from dynamics and symmetry, submitted to *Phys. Rev. Lett.*, 1980.

19. J. Guckenheimer, Bifurcation and catastrophe, in *Dynamical Systems*, M. M. Peixoto, Ed., Academic, New York, NY, 1973, 95–110.
20. J. Guckenheimer, A strange strange attractor, *The Hopf Bifurcation*, Marsden and McCracken, Eds., Appl. Math. Series 19, Springer-Verlag, Berlin, 1976, 368–381.
21. W. Güttinger and H. Eikemeier (Eds.), *Structural Stability in Physics*, Synergetics Vol. 4, Springer-Verlag, Berlin, 1979.
22. J. Hayden and E. C. Zeeman, 1980 Bibiliography on catastrophe theory, Univ. Warwick, Coventry.
23. M. Hénon, A two-dimensional mapping with a strange attractor, *Commun. Math. Phys.* **50** (1976), 69–77.
24. P. J. Holmes, A non-linear oscillator with a strange attractor, *Phil. Trans. Roy. Soc.* **292** (1979), 419–448.
25. E. Hopf, Abzweigung einer periodischen Lösung von einer stationären Lösung einer Differentialsystems, *Ber. Verh. Sachs. Akad. Wiss. Leipzig Math. Phys.* **95** (1943), 3–22.
26. L. D. Landau and E. M. Lifshitz, *Fluid Mechanics*, Pergamon, Oxford, 1959.
27. E. Looijenga, On the semi-universal deformation of a simple-elliptic singularity, Part I: Unimodularity, *Topology*, **16** (1977), 257–262.
28. E. N. Lorenz, Deterministic nonperiodic flow, *J. Atmos. Sci.* **20** (1963), 130–141.
29. R. Lozi, Un attracteur étrange (?) du type attracteur de Hénon, *J. Phys.* **39**, C5 (1978), 9–10.
30. L. Markus, *Lectures in Differentiable Dynamics*, CBMS Regional Conf. Ser. in Math. 3, Amer. Math. Soc., Providence, RI, 1971; revised 1980.
31. L. Markus, Extension and interpolation of catastrophes, *Ann. NY Acad. Sci.* **316** (1979), 134–149.
32. J. E. Marsden and M. McCraken, *The Hopf Bifurcation and Its Applications*, Applied Math. Series 19, Springer-Verlag, Berlin, 1976.
33. J. Mather, Stability of C^∞-mappings, *Publ. Math. IHES* **35** (1968), 127–156 and **37** (1969), 223–248.
34. M. Misiurewicz, Strange attractors for Lozi mappings, in *Proc. Symp. Dynamical Systems & Turbulence*, Warwick 1980, Lecture Notes in Math., Springer-Verlag, Berlin (to appear).
35. A. S. Monin, On the nature of turbulence, *Sov. Phys. Usp.* **21**, 5 (1978), 429–442.
36. S. Newhouse and J. Palis, Bifurcations of Morse–Smale dynamical systems, in *Dynamical systems*, M. M. Peixoto, Ed., Academic, New York, NY, 1973, 303–366.
37. S. Newhouse, Diffeomorphisms with infinitely many sinks, *Topology* **13** (1974), 9–18.
38. S. Newhouse, D. Ruelle, and F. Takens, Occurrence of strange Axiom *A* attractors near quasi periodic flows on T^m, $m \geq 3$, *Commun. Math. Phys.* **64** (1978), 35–40.
39. J. Palis and S. Smale, Structural stability theorems, *Global Analysis*, Proc. Symp. Pure Math. 14, Am. Math. Soc., Providence, RI, 1970, 223–231.
40. W. Parry, Cocycles and velocity changes, *J. Lond. Math. Soc.* (2) 5 (1972) 511–516.
41. Ja. B. Pesin, Lyapunov characteristic exponents and smooth ergodic theory. *Russian Math. Surveys* **32**, 4 (1977), 55–114.
42. R. V. Plykin, Sources and currents of *A*-diffeomorphisms of surfaces, *Math. Sb.* **94**, 2(b) (1974), 243–264.
43. T. Poston and I. N. Stewart, *Catastrophe Theory and Its Applications*, Pitman, London, 1978.
44. C. C. Pugh and M. Shub, The Ω-stability theorem for flows, *Invent. Math.* **11** (1970), 150–158.

45. D. Rand, The topological classification of Lorenz attractors, in *Proc. Camb. Phil. Soc.* **83** (1978), 451–460.
46. —, Dynamics and symmetry: Predictions for modulated waves in rotating fluids, *Arch. Rat. Mech.*, to appear.
47. D. Rand and E. C. Zeeman, Models of the transition to turbulence in certain hydrodynamical experiments, in *Proc. Symp. Dynamical Systems & Turbulence, Warwick 1980*, Lecture Notes in Maths, Springer-Verlag, Berlin, to appear.
48. J. Robbin, A structural stability theorem, *Ann. Math.* **94** (1971), 447–493.
49. R. C. Robinson, Structural stability of vector fields, *Ann. Math.* **99** (1974), 154–175.
50. O. E. Rössler, Chaos, *Structural Stability in Physics*, W. Güttinger and H. Eikemeier, Eds., Synergetics Vol. 4, Springer-Verlag, Berlin, 1979, 290–309.
51. D. Ruelle and F. Takens, On the nature of turbulence, *Comm. Math. Phys.* **20** (1971), 167–192 and **23** (1971), 343–344.
52. D. Ruelle, A measure associated with Axiom *A* attractors, *Amer. J. Math.* **98** (1976), 619–654.
53. —, The Lorenz attractor and the problem of turbulence, in *Quantum Dynamics Models and Mathematics*, Lecture Notes in Math. Vol. 565, Springer-Verlag, Berlin, 1976, 146–158.
54. —, Sensitive dependence on initial condition and turbulent behaviour of dynamical systems, *Ann. NY Acad. Sci.* **316** (1978), 408–416.
55. —, Les attracteurs étranges, *La Recherche* **108**, 11 (1980), 132–144.
56. —, Ergodic theory of differentiable dynamical systems, *Publ. Math. IHES* **50**, 1979, 27–58.
57. —, On the measures which describe turbulence, preprint, IHES, 1978.
58. D. Schaeffer, Qualitative analysis of a model for boundary effects in the Taylor Problem, *Math. Proc. Camb. Phil. Soc.* **87** (1980), 307–337.
59. F. J. Seif, Cusp bifurcation in pituitary thyrotropin secretion, in *Structural Stability in Physics*, W. Güttinger and H. Eikermeier, Eds., Synergetics Vol. 4, Springer-Verlag, Berlin, 1979, 275–289.
60. R. Shaw, Strange attractors, chaotic behaviour, and information flow, Preprint, Univ. Cal., Santa Cruz, 1978.
61. M. Shub, Thesis, Univ. California, Berkeley, 1967.
62. S. Smale, A structurally stable differentiable homeomorphism with an infinite number of periodic points, in *Proc. Int. Symp. Non-linear Vibrations, Vol. II*, 1961; *Izdat. Akad. Nauk Ukrain, Kiev* (1963), 365–366.
63. —, Diffeomorphisms with many periodic points, *Differential and Combinatorial Topology*, Princeton Univ. Press, Princeton, NJ, 1965, 63–80.
64. —, Differential dynamical systems, *Bull. Amer. Math. Soc.* **73** (1967), 747–817.
65. —, The Ω-stability theorem, *Global Analysis*, Proc. Symp. Pure Math. Vol. 14, Am. Math. Soc., Providence, RI, 1970, 289–298.
66. —, Dynamical systems and turbulence, in *Turbulence Seminar*, Lecture Notes in Math. Vol. 615, Springer-Verlag, Berlin, 1977, 48–70.
67. H. L. Swinney and J. P. Gollub, The transition to turbulence, *Physics Today*, **31**, 8 (1978), 41–49.
68. F. Takens, Unfoldings of certain singularities of vector fields: Generalised Hopf bifurcations, *J. Diff. Eqs.* **14** (1973), 476–493.
69. —, Singularities of vector fields, *Publ. Math. IHES* **43** (1974), 47–100.
70. —, Detecting strange attractors in turbulence, in *Proc. Symp. Dynamical Systems and Turbulence, Warwick 1980*, Lecture Notes in Math., Springer-Verlag, Berlin, to appear.
71. G. I. Taylor, Stability of a viscous liquid contained between two rotating cylinders, *Phil. Trans. Roy. Soc. A* **223** (1923), 289–343.

72. R. Thom, *Structural Stability and Morphogenesis* (Engl. trans. D. Fowler, 1975) Benjamin, New York, NY, 1972.
73. —, Structural stability, catastrophe theory and applied mathematics, *SIAM Review* **19** (1977), 189–201.
74. R. F. Williams, Expanding attractors, *Publ. Math. IHES* **43** (1974), 161–203.
75. —, The structure of Lorenz attractors, *Publ. Math. IHES*, **50** (1979), 73–100.
76. E. C. Zeeman, *Catastrophe Theory: Selected Papers 1972–1977*, Addison-Wesley, Reading, MA, 1977.